Footprint, Weathering, and Persistence of Synthetic-Base Drilling Mud Olefins in Deep-Sea Sediments following the Deepwater Horizon Disaster

Scott A. Stout[a*] and James R. Payne[b]

[a] NewFields Environmental Forensics Practice, LLC, 300 Ledgewood Pl., Suite 305, Rockland, MA
[b] Payne Environmental Consultants, Inc. 1651 Linda Sue Ln., Encinitas, CA

Abstract

Olefin-based synthetic-based drilling mud (SBM) was released into the Gulf of Mexico as a result of the *Deepwater Horizon* (DWH) disaster in 2010. We studied the composition of neat SBM and, using conventional GC-FID, the extent, concentration, and chemical character of SBM-derived olefins in >3600 seafloor sediments collected in 2010/2011 and 2014. SBM-derived (C_{14}-C_{20}) olefins occurred (up to 10 cm deep) within a 6.5 km^2 "footprint" around the well. The olefin concentration in most sediments decreased an order of magnitude between 2010/2011 and 2014, at least in part due to biodegradation, evidenced by the preferential loss C_{16} and C_{18} linear (α- and internal) versus branched olefins. Based on their persistence for 4-years in sediments around the Macondo well, and 13-years near a former unrelated drill site (~62 km away), weathered SBM-derived olefins released during the DWH disaster are anticipated to persist in deep-sea sediment for (at least) a comparable duration.

Keywords:
Oil spill, alkenes, biodegradation, Macondo, recovery, drilling fluid

*corresponding author: Tel.: +1 781 681 5040; e-mail: sstout@newfields.com

1.0 Introduction

Synthetic-based drilling muds (SBMs) are man-made fluids commonly used in drilling oil and gas wells. SBMs provide lubricity, stability at high temperatures, and borehole stability especially in more difficult to drill deepwater and directional wells. In addition, SBMs offer an advantage over oil-based (diesel) muds (OBMs) in terms of the potential environmental issues surrounding their accidental or intentional discharge to the environment because SBMs are designed to be less toxic and degrade faster in marine sediments (Neff et al., 2000; Am. Chem. Council, 2006). SBMs are generally comprised of 30 to 90 % volume (20-50 wt%) of synthetic organic compounds, which act as lubricants, that are dispersed in a salt brine to form an emulsion, along with other ingredients including emulsifiers, barite, clays, lignite, or lime. The most common synthetic organic compounds in SBMs are monounsaturated acyclic hydrocarbons, i.e., olefins (C_nH_{2n}). Other more rarely used synthetic hydrocarbons include linear alkyl benzenes (LABs) and synthetic paraffins (ethers and esters).

The synthetic olefins can occur in a variety of forms, *viz.*, linear α-olefins (LAOs), internal olefins (IOs) or, less commonly, poly α-olefins (PAOs). LAOs are formed by the catalytic oligomerization of ethylene (C_2H_4) to produce olefins containing a double bond in the α-position and, owing to the ethylene monomer, are dominated by compounds containing an even number of carbons between 8 (C_8H_{16}) to 20 ($C_{20}H_{40}$), which are subsequently distilled to yield LAO blends of varying carbon range. The distilled LAO blends used in SBMs typically contain 14 to 20 carbons. IOs are formed by the catalytic isomerization of LAOs that shifts the double bond from the α-position to some internal position along the carbon chain. As such, numerous IO isomers can be formed depending on the position of the double bond. IOs used in SBMs typically also are distilled to contain 15 to 20 carbons (Am. Chem. Council, 2006). Although dominated by straight-chain (linear) isomers, both LAOs and IOs will contain some, mostly methyl-, branched olefin isomers (MBOs) that presumably form as by-products in the synthesis of LAOs and IOs. MBOs reportedly comprise 15 to 40 percent of LAO and IO blends (Am. Chem. Council, 2006). LAO and IO blends can be used separately, or more commonly, are blended together to produce desired physical properties important for drilling (Neff et al., 2000). As such, most commercial SBMs contain a complex mixture

of LAO and IO isomers, with smaller amounts of PAOs and/or MBOs, all of which are dominated by even-carbon numbered isomers in the C_{14} to C_{20} range.

Although olefins are not found in most crude oils, trace amounts of LAOs and IOs (termed terminal and *trans*-olefins in oil chemistry literature, respectively) are sometimes formed in crude oil due to (1) radiolytic dehydrogenation of saturated hydrocarbons induced by radioactive elements in reservoir minerals or (2) oil cracking caused by the thermal stress due to igneous intrusions (Curiale and Frolov, 1998). The abundance and distributions of these naturally-occurring olefins in crude oil are completely unlike the concentrated "clusters" of C_{14} to C_{20} olefin isomers found in SBM. As such, a prominence of clusters of C_{14} to C_{20} olefin isomers in marine sediments clearly indicates an impact by olefin-based SBMs in those sediments, and not crude oil.

SBM is not typically discharged in bulk to the environment. However, rock cuttings containing traces of adhered SBM are routinely discharged and multiple seafloor studies have assessed the impact of LAOs and IOs from SBM on deep-sea sediments (Neff et al., 2000; OGP, 2003; CSA, 2004a,b). These studies on the conventional discharge of SBM associated with rock cuttings have collectively concluded that high concentrations (>10,000 μg/g) of synthetic olefins were typically only observed within 100 to 250 m of the drilling platform and occasionally up to 1 to 2 km from the well depending upon ocean currents. In addition, the concentration of synthetic olefins measured in sediments decreased over time, mostly within 1 to 2 years of discharge, which was attributed to a combination of resuspension, bed transport, mixing (bioturbation), and biodegradation. The rate of decrease, however, is difficult to document because of the typically heterogeneous distribution of cuttings in sediments. Nonetheless, the impact of SBM on deep-sea sediments is conventionally thought to be both spatially and temporally constrained.

A commercial SBM, known as *Rheliant* (manufactured by MiSWACO), was being used in the drilling of the failed Macondo well in ~1,500 m of water prior to the *Deepwater Horizon* (DWH) disaster and oil spill (BP, 2010). In the moments prior to and during the blowout, the SBM within the well was expelled at the drill rig and, upon failure of the riser pipe, also into the deep-sea in bulk along with the escaping gas and crude oil. The more than 2,200 barrels (bbl) of SBM that was within the hole and drill string system as

the blowout occurred (BP, 2010), plus any bulk SBM in storage containers and pits on the sinking drilling rig, were ultimately spilled or carried to the seafloor ~1,500 m below. In the course of the spill's Response efforts, SBM also was used in the failed Top Kill operation conducted during the active spill (May 26-29, 2010), during which nearly 30,000 bbl of SBM – at times including various bridging materials (e.g., golf balls, cubes, and miscellaneous objects; Junk Shot) – were pumped at rates up to 80 bbl/min into the failed well in an attempt to stop or reduce the flow of oil and gas (DOE, 2014). After three attempts over three days, the Top Kill operation was considered unsuccessful and abandoned. Some unknown volume of SBM used during the operation was also released into the deep-sea in bulk. SBM was also used during the Static Kill operation conducted after the well was shut-in (August 3-5, 2010) in an effort to push any remaining oil within the well back into the reservoir.

The collective impact that these bulk (non-conventional) discharges of SBM into the deep-sea during the initial blowout, rig sinking, and response operations had on the sediments located around the Macondo well is largely unknown – and, of course, was not independent of the impact of the crude oil discharged during the spill. Potential impacts to the benthos include smothering, toxicity of the SBM components, and depletion of oxygen during biodegradation.

In this study, the chemical compositions of the SBMs associated with the DWH incident are reviewed and their chemical fingerprints are presented and compared to more than 3,600 sediments collected from the seafloor (Stout et al., 2016). Evidence is presented showing the concentration, spatial distribution, and molecular character of SBM-derived olefins in deep-sea surface and subsurface sediments around the failed Macondo well in 2010-2011 and again in 2014, four years after the DWH incident. In addition, sediments collected near a former drill site 62 km northeast of the study area show the persistence of weathered SBM-derived olefins for more than 13 years, indicating those present in sediments near the failed Macondo well are anticipated to persist for (at least) a comparable duration.

2. Samples and Methods

2.1 Synthetic-Based Drilling Muds

Six neat samples of SBMs were provided by BP for this study (Table 1). Five of these were characterized as Top Kill muds obtained from four different sources/vessels on June 2, 2010, approximately 1 week after the Top Kill/Junk Shot operation (Table 1). One additional SBM sample was obtained from another vessel, *viz*., the *HOS Centerline*, on June 26, 2010 approximately 1 month after the Top Kill/Junk Shot operation. However, this additional sample was notable because the *HOS Centerline* was reportedly the primary vessel in use during Top Kill/Junk Shot operation – and was later used in the Static Kill operation in early August. The SBM obtained from the *HOS Centerline* was indicated to be comprised of *Encore* SBM, a product of Halliburton. We consider this sample to best represent the mud used during the Top Kill/Junk shot operation, and perhaps during the Static Kill operation. No sample of the *Rheliant* SBM in use during the initial blowout was available for study. All six SBM samples were shipped to Alpha Analytical Laboratory (Alpha; Mansfield, Massachusetts) under full chain-of-custody in September 2010.

2.2 Sediment and Slurp Gun Filter Samples

Deep-sea sediment cores were collected between September 2010 and October 2011, herein referred to as 2010/2011, and again in May and June 2014 as part of the NRDA following the *Deepwater Horizon* oil spill. A total of 2,782 sediment samples from 724 cores were collected in 2010/2011 and 830 sediment samples from 201 cores were collected in 2014. These cores were sub-sampled and analyzed at a relatively high-resolution wherein surface intervals (0-0.5, 0-1, 0-1.5, and 0-2 cm) and between two and seven individual deeper intervals were isolated for study within the (mostly) 10 cm cores. The sediment intervals analyzed in the majority of the 2010/2011 and 2014 cores were 0-1, 1-3, 3-5, and 5-10 cm. These intervals were carefully isolated onboard the sampling vessels shortly after collection and placed in glass jars and frozen prior to being shipped cold to Alpha under full chain-of-custody.

In addition, in April 2011 a novel vacuum system (slurp gun) mounted on a remotely operated vehicle (ROV) was used to collect eight SBM-enriched “fallout” samples onto glass fiber filters (Payne and Driskell, 2015; Stout et al., 2016). These slurp gun filter samples were collected at eight stations along three of six parallel SE-NW transects south of the wellhead (Fig. S-1). The ROV was “flown” 0.5-1.0 m above the bottom at

0.5 knots along all six transects for continuous visual observations and photographic documentation. Where anomalous and ubiquitous deposits of SBM-enriched "fallout" were observed (mostly along transects within 2 km of the wellhead; Fig. S-1) eight samples were "surgically" vacuumed from the seafloor with the aid of on-board closed-circuit TV signals in the ROV control room. As with the sediment cores, the SBM-enriched slurp gun filter samples were immediately frozen on board and shipped cold to Alpha under full chain-of-custody.

Additional details surrounding the sediment and slurp gun filter samples were previously described in Stout et al. (2016), in which the distribution and chemical character of Macondo oil throughout the deep-sea floor up to 30 km from the well was discussed. In the present study, we emphasize the presence and chemical character of SBM-derived synthetic olefins in the 2010/2011 and 2014 sediment samples and April 2011 slurp gun filters that were recognized to contain synthetic olefins using conventional gas chromatography-flame ionization detection (GC-FID; see below).

2.2 Sample Preparation

Following homogenization by sonication or mixing, respectively, aliquots of the neat SBMs (Table 1) and sediment samples (~10 and 30 g wet, respectively) and each whole slurp gun filter sample were spiked with recovery internal surrogates (RIS; 5α-androstane, acenaphthene-d_{10}, chrysene-d_{12}), dried with anhydrous Na_2SO_4 and serially-extracted (3-times; 6, 2, and 0.5 hrs) using 100 mL fresh dichloromethane (DCM) on a shaker table. The serial extracts from each sample were combined, filtered through glass wool, dried with anhydrous Na_2SO_4, concentrated to 1 mL using Kuderna Danish apparatus and nitrogen blow-down. Sediment extracts were further treated with activated copper to remove sulfur, and silica gel-cleaned using EPA Method 3630C, re-concentrated to 1 mL (as above). The concentrated extracts of SBMs, sediments, and slurp gun filters were spiked with surrogate internal standards (SIS; *o*-terphenyl, *n*-tetracosane-d_{50}, 2-methylnaphthalene-d_{10}, pyrene-d_{10}, benzo(b)fluoranthene-d_{12}, and 5β(H)-cholane) prior to instrument analysis.

2.3 Instrument Analysis

All sample extracts were analyzed using a modified EPA Method 8015B described in detail elsewhere (Douglas et al., 2015). The method was conducted via conventional 1-

dimensional GC-FID; Agilent 6890) equipped with a Restek Rtx-5 (60m x 0.25 mm ID, 0.25 μm film) fused silica capillary column. Extracts were injected (1 μL, pulsed splitless) into the GC programmed from 40°C (1 min) and ramped at 6°C/min to 315°C (30 min) using H_2 (~3 mL/min) as the carrier gas. Prior to sample analysis a minimum five-point calibration was performed to demonstrate the linear range of the analysis. The calibration solution was composed of selected aliphatic hydrocarbons within the *n*-C_9 to *n*-C_{40} range. Analyte concentrations in the standard solutions ranged from 1 ng/μL to 200 ng/μL. All calibration solution compounds that fall within the window were used to generate the average response factor for TPH and TPH_{SBM} quantification (Section 2.4).

2.4 Quantification of TPH and TPH_{SBM}

GC-FID analysis was used to determine the concentrations of GC-amenable total petroleum hydrocarbons (TPH) defined as the total mass eluting between n-C_9 and n-C_{44} (exclusive of internal standards and after blank subtraction) in all samples. In addition, the concentration of TPH attributable to synthetic olefins in the *n*-C_{14} to *n*-C_{20} range, herein termed TPH_{SBM}, was also determined. For the neat SBMs, TPH_{SBM} was determined by individually integrating the areas representing each C_{14} to C_{20} olefin-containing "cluster". The percent of each cluster was determined individually and the total area of the clusters (ΣC_{14}-C_{20}) was used to determine the TPH_{SBM} in the neat samples. In the case of sediments and slurp gun filter samples, the total area resolved peaks spanning the C_{14} to C_{20} olefin clusters was first integrated. For those samples that also contained Macondo crude oil, peak areas attributable to C_{14} to C_{20} *n*-alkanes and acyclic isoprenoids (*viz.*, 2,6,10-trimethytridecane, norpristane, pristane or phytane) that eluted within the targeted olefin clusters were excluded from the calculation of TPH_{SBM}. Similarly, any mass within the olefin clusters represented by any crude oil-derived unresolved complex mixture (UCM) was excluded. Thus, only the chromatographic areas representing olefins within the C_{14} to C_{20} resolved olefin clusters were used in calculating the concentration of TPH_{SBM} in sediment and slurp gun filter samples. The weight percent of the (total) TPH occurring as TPH_{SBM} in deep-sea sediment and slurp gun filters containing SBM-derived olefins was calculated [(TPH_{SBM}/TPH) x 100]. The TPH and TPH_{SBM} concentrations in the neat SBM, sediment, and slurp gun filter samples are reported in μg/g, μg/g_{dry}, and μg/filter, respectively. Because TPH concentrations of the slurp gun filter samples were dependent upon the

mass of particles collected on each filter, these results were used primarily to assess the chemical fingerprints of the SBM-enriched particles and not their absolute concentrations on the seafloor.

3. Results and Discussion

3.1 Chemical Character of Neat SBMs

Table 1 contains the tabulated results obtained for the neat SBMs studied. The concentration of TPH in the samples widely ranged from non-detect to 990,000 μg/g (99 wt%). [Recall the denominators in these concentrations represent the weight of the total SBM sample, which included non-hydrocarbon components such as barite.] This large range was surprising considering the synthetic hydrocarbon component of SBMs are expected to comprise approximately 20 to 50 wt% of SBMs (Neff et al., 2006), or 200,000 to 500,000 μg/g. Only two of the SBMs studied contained TPH in this approximate range (40 and 54 wt%), while three samples contained much less (nd to 6.5 wt%), and one contained nearly "pure" (99 wt%) synthetic hydrocarbons (Table 1). We attribute this broad and irregular range in TPH to the heterogeneity imparted during the original sampling of the SBMs from the vessels. As noted in Table 1's footnotes, the tanks used to store the SBMs were intermittently stirred, a process intended to maintain the mixture of dense inorganic constituents (e.g., barite) with less dense organics (e.g., olefins). We hypothesize that the samples' collection times, relative to the most recent stirring interval, as well as the sample depths within the tanks, affected the composition of the SBM samples provided for study. For example, gravitational downward settling of the barite and floating of the hydrocarbon components of the SBMs might be expected to commence and progressively occur following the end of a stirring event. Thus, both the time since the last stirring event and the depth from which the sample was collected likely varied among the samples studied. For example, the high TPH concentration of *HOS Centerline* SBM (99 wt%) and low TPH concentration in the *Carol Chouest* SBMs (nd) could reflect such differences, with the former hypothetically being collected from near the top of the tank just prior to a stirring event and the latter hypothetically being collected deep in the tank just prior to a stirring event. Unfortunately, there is no record of when stirring events occurred relative to the sampling times (Table 1).

Between 86 and 93 wt% of the TPH in the three SBMs that had contained elevated concentrations of TPH (see Table 1, bottom) consists of olefins in the C_{14} to C_{20} range. Oppositely, a small wt% (7 to 14) of the SBMs' total extractable hydrocarbons occurs outside the C_{14} to C_{20} range. Inspection of these samples' corresponding GC-FID chromatograms (Fig. 1) indeed reveals a predominance of peaks occurring within seven olefin "clusters" throughout the 14 to 20 carbon range (Fig. 1). However, the *Infant Jesus* SBM contains a small cluster of peaks around C_{13} and also a very small unresolved complex mixture (UCM) hump in the C_{25+} range (Fig. 1A). The *Kylie Williams* and *HOS Centerline* SBMs do not contain any C_{13} range cluster or UCM, but do each contain four resolved peaks beyond C_{20} that occur in highly consistent proportions (see starred peaks; Figs. 1B-C). Based upon GC-FID retention time comparison to biodiesels containing multiple fatty acid methyl esters (confirmed by full-scan GC-MS) analyzed in our lab, these four peaks are identified to be an even-carbon homologous series of (C_{18}, C_{20}, C_{22} and C_{24}) fatty acid methyl esters (FAMEs) containing one or two C-C double bonds. Their presence is not surprising as these esters are sometimes included in SBM blends to achieve certain drilling properties (Neff et al., 2000).

As anticipated, the GC-FID chromatograms of the SBMs are clearly dominated by the four olefin clusters in the C_{15} to C_{18} range (Fig. 1). The individual peaks within each cluster are comprised of the single α-olefin and numerous internal olefin (IO) and methyl-branched olefin (MBO) isomers, as is typical of olefin-based SBMs (Neff et al. 2000; Reddy et al. 2007). Also as expected, the clusters around C_{16} and C_{18}, i.e., even-carbon numbers, are dominant owing to their production via the polymerization of ethylene (C_2H_4) whereas the clusters around C_{15} and C_{17} are smaller (Fig. 1). Distillation of the SBMs' original blend stocks results in much lower amounts of C_{13}, C_{14}, C_{19} and C_{20} olefins (Fig. 1).

The relative abundances of the four dominant (C_{15} to C_{18}) olefin clusters were somewhat variable among the five SBMs in which they could be measured (Table 1). For example, the *Kylie Williams* SBM contained lower proportions of C_{16} (41%) and C_{18} (26%) olefins compared to the *Infant Jesus* and *HOS Centerline* SBMs (46-47% and 31-32%, respectively), a difference also visually evident in these samples' chromatograms (Fig. 1). This type of variability cannot reasonably be attributed to heterogeneities brought

about by density-driven separation following stirring events within the tanks (as with the variable absolute TPH concentrations described above). Instead, the variations among the percentages of the different olefin clusters in these neat SBMs reflect true differences in their original SBM formulations. This variation indicates that the SBMs collected from the different vessels were not derived from a single SBM blend, but rather represented a variety of similar SBM formulations. On average (± 1σ), the weight percent of the C_{14} to C_{20} olefin clusters in the five SBMs in which these could be measured were 1 ± 2 (C_{14}), 12 ± 3 (C_{15}), 41 ± 6 (C_{16}), 11 ± 3 (C_{17}), 31 ± 3 (C_{18}), 2 ± 0.4 (C_{19}), and 1 ± 0.4 (C_{20}; Table 1).

The olefin clusters in the *HOS Centerline* SBM are shown expanded in Fig. 2. (Expanded views of the *Infant Jesus* and *Kylie Williams* SBMs from Fig. 1A and B are shown in Fig. S-2 of the *Supporting Information*.) As noted above, there are many co-eluting and overlapping peaks present within each cluster. Based upon general compositions of SBM (e.g., Neff et al. 2000), each cluster would be predicted to include each carbon number's linear α-olefin (LAO) as well as multiple internal olefin (IO) isomers and/or methyl-branched olefin (MBO) isomers. Molecular structures indicate there are six IO and seven MBO isomers possible in the C_{15} cluster, seven IO and seven MBO isomers possible in the C_{16} cluster, seven IO and eight MBO isomers possible in the C_{17} cluster, and eight IO and eight MBO isomers possible in the C_{18} cluster. Thus, a total of 14 to 17 olefin isomers are possible within the C_{15} to C_{18} clusters.

Inspection reveals that each cluster exhibits a comparable pattern of peaks, with the notable exception of additional series of overlapping peaks eluting at the front of both the C_{16} and C_{18} (and possibly C_{20}) olefin clusters (Fig. 2). Based upon GC-FID retention time comparison for selected LAO reference standards (1-hexadecene and 1-octadecene) the identity of the α-olefin in each cluster is indicated to elute just ahead of where *n*-alkanes normally elute (Fig. 2). In addition, Aeppli et al. (2013), who had analyzed aliquots of these same six neat SBMs using GC x GC-FID and GC x GC-TOF/MS similarly confirmed the elution/identity of a single LAO but also the presence of multiple IO and MBO isomers within each cluster. The elution order and magnitude of peaks reported by Aeppli et al. (2013) and observed herein are virtually identical, allowing us to identify peaks attributable to IO and MBO isomers within each cluster (Fig. 2). Interestingly the most prominent IO isomers – arbitrarily labelled a, b, and c

(Fig. 2) – occur in a similar pattern in each of the SBMs with isomers a and b exceeding isomer c within each isomer cluster (Figs. 2 and S-2). The earlier eluting of these three IO isomers (peak a) elutes at the same retention time as the corresponding *n*-alkane using conventional 1-dimensional GC employed herein; see arrows indicating *n*-alkane elution time in Fig. 2). However, using 2-dimensional GC x GC Aeppli et al. (2013) confirmed the absence of *n*-alkanes, pristane, and phytane among each of the olefin clusters (despite their co-elution with olefins). Finally, as noted above, groups of small overlapping peaks elute at the front of both the C_{16} and C_{18} clusters (only; Fig. 2). These earlier-eluting peaks are determined to be various MBO isomers (Fig. 2) based on the fact that these compounds remained resolved and eluted in front of *n*-alkanes after the olefins in the SBMs were hydrogenated (Aeppli et al., 2013). Thus, like Aeppli et al., we have similarly identified these peaks as MBOs (Figs. 2 and S-2). The fact that these MBOs exist only within the C_{16} and C_{18} (and perhaps C_{20}) olefin clusters is interesting. Reddy et al. (2007) similarly had identified C_{16} and C_{18} MBOs (only) in an SBM-impacted oil (unrelated to DWH) using GC x GC. The presence of C_{16} and C_{18} MBOs (only) likely reflects some unique oligomerization pathway(s) in the synthesis of olefins that produces only the even-carbon MBOs.

3.2 SBM in Deep-Sea Sediments in 2010/2011

Despite the detailed isomer differences among the neat SBMs studied, the distinctive chromatographic appearance of the olefin clusters in all the SBMs (Figs. 1 and 2) made their presence easy to recognize within the GC-FID chromatograms of hydrocarbons extracted from the deep-sea sediments studied. In 2010/2011, 2,782 deep-sea sediment samples from 724 cores were collected and analyzed using conventional 1-dimensional GC-FID (Section 2.3). Each of these sediment's GC-FID chromatograms was qualitatively inspected for the presence of the C_{14} to C_{20} (mostly C_{16} and C_{18}) olefin clusters indicative of impact by SBM-derived olefins. The chromatograms of those sediment samples in which olefin clusters were recognized were integrated (Section 2.4) to determine the relative abundance of the TPH that was attributed to the C_{14} to C_{20} olefins (TPH_{SBM}). It is acknowledged that at some low concentration of olefins their presence in sediments containing crude oil might go unrecognized using conventional GC-FID. Therefore, we consider this approach to recognizing and quantifying SBM-derived olefins impact on deep-sea sediments, especially crude oil-impacted sediments,

as being conservative since only those sediments whose GC-FID chromatograms obviously revealed visible olefin clusters were quantified. Notably, however, in sediments not containing prominent crude oil we were able to qualitatively recognize SBM-derived olefin clusters at TPH_{SBM} concentrations of only a few $\mu g/g_{dry}$ (see below).

Among the 2,782 sediments from 2010/2011 analyzed a total of 143 sediments (~5%) were determined to contain SBM-derived olefins. An inventory of these 143 samples is provided in Table S-1 of the *Supporting Materials*. Most of these sediments (118) were obtained from multiple sediment depth intervals (0-1, 1-3, 3-5, and 5-10 cm) in 40 cores collected within 2.3 km of the Macondo well (Fig. 3). The olefins in these proximal sediments were undoubtedly attributed to the DWH incident as they co-occurred with varying amounts Macondo oil (described below). Notably, 40 of the 47 total cores collected within 2.3 km of the well in 2010/2011 contained the SBM-derived olefins; those seven cores not containing olefins were collected at the periphery of the cores in this area (Fig. 3). The near pervasive presence of SBM-derived olefins in sediments around the well indicates that SBM was deposited in all cardinal directions around the failed well, although its deposition extended slightly further in a southwesterly direction (Fig. 3). SBM deposition 3.7 km toward the northeast was also evident in one core location, although the continuity of deposition in this direction is uncertain owing to a lack of cores collected between the Macondo well and this one location (Fig. 3). Ignoring this single core 3.7 km away, the SBM-derived olefins "footprint" resulting from the DWH incident in 2010/2011 was conservatively depicted to cover approximately 6.5 km^2 of the seafloor around the Macondo well (Fig. 3). This size "footprint" contrasts with the results of previous seafloor sediment studies unrelated to DWH that showed most SBM-impacted sediments existed within 250 m (i.e., ~0.2 km^2) of their discharge point, although these studies focused on shallower water drill sites where SBM was conventionally discharged (<556 m; CSA, 2004a,b). The larger "footprint" around the failed Macondo well likely resulted from (at least in part) the bulk and catastrophic discharge(s) of the hydrophobic neat SBM, as opposed to the conventional discharge of "fast-sinking" SBM-laden ("oil-wet") rock cuttings during normal drilling operations, which allowed for a greater dispersion of the SBM-derived olefins in sediments around the Macondo well. The significant water depth of the Macondo well (~1500 m) also likely facilitated greater dispersion of any SBM discharged at/near the sea surface.

Notably, the remaining 25 of the 143 sediments recognized to contain SBM-derived olefins that occurred in sediments collected further from the wellhead (up to 62 km to the northeast) and which did not co-occur with Macondo oil, are not reasonably attributed to the DWH incident. Rather, these remote occurrences of SBM-derived olefins in deep-sea sediments are more reasonably attributed to past drilling operations and the conventional discharge of SBM-bearing cuttings to the seafloor. These samples are listed separately at the bottom of Table S-1 and are discussed further in Section 3.5.

Fig. 4 shows the GC-FID chromatograms for four deep-sea surface (0-1 cm) sediments collected near the Macondo well in 2010/2011 impacted by SBM-derived olefins. The presence of the olefin clusters in the C_{15} to C_{18} range, each being dominated by the C_{16} olefins, such as was evident in the neat SBMs (Figs. 1 and 2), are easily recognized in the chromatograms for each of the samples. Nearly all of the 2010/2011 sediments that contained SBM-derived olefins also contain some Macondo oil, as evidenced by the presence of *n*-alkanes and a broad unresolved complex mixture (UCM) extending up to around C_{40}. However, the proportions of crude oil and SBM-derived olefins varied widely, as demonstrated by these four samples' chromatograms. Some sediments contained only a small percentage SBM-derived olefins mixed with crude oil (7 wt%; Fig. 4A) whereas other sediments contained almost exclusively C_{14} to C_{20} SBM-derived olefins (96 wt%; Fig. 4D). In the latter, the small balance (4 wt%) consisted of C_{11} to C_{14} *n*-alkanes, which though not quantified as TPH_{SBM} are likely associated with SBM rather than with oil (discussed below). Notably, outside of the 2.6 km^2 SBM "footprint" (Fig. 3), severely weathered Macondo oil residues were found up to 30 km from the well (Stout et al., 2016), indicating that the area of the seafloor impacted by SBM from the DWH incident was much smaller than that impacted by the spilled oil. This difference is attributed to the more prolific transport of (chemically and physically) dispersed oil droplets within the deep-sea advective layer that had formed ~200 to 500 m above the wellhead (e.g., Camilli et al., 2010; Socolofsky et al., 2011; Spaulding et al., 2015) and served to laterally transport oil far from the well. SBM-derived olefins, on the other hand, were not as widely distributed by the deep-sea plume perhaps owing to their association with denser (barium-bearing) particles in the spilled SBM(s) that were not as susceptible to lateral transport within the deep-sea advective layer.

The homologous series of four FAMEs that eluted beyond C_{20} in some of the neat SBMs (starred peaks in Fig. 1B-C) were rarely observed in any of the sediments containing SBM-derived olefins (e.g., see Fig. 4C). The absence of FAMEs in most SBM-impacted sediments collected in 2010/2011 may, in part, be due to the inability to clearly see these peaks when SBM co-occurs with crude oil in sediments. In addition, because FAMEs are somewhat polar and more water-soluble than olefins, they may have preferentially dissolved into seawater (before or after SBM deposition) and/or biodegraded more rapidly than olefins.

There was no relationship between the TPH concentration attributable to crude oil (TPH-TPH_{SBM}) and the TPH_{SBM} concentration (r^2 = 0.10; from Table S-1), which argues that SBM-derived olefins were deposited independently of the crude, i.e., all of the oil and all of SBM-derived olefins did not necessarily "travel together" to reach the seafloor. This contention is supported by the visual observations made during the ROV transects completed on the *HOS Sweet Water* 2 Leg 2 cruise in April 2011 (Fig. S-1). Tungsten lamps on the ROV revealed an abundance of white, "star-like" clusters on the seafloor (Fig. 5A) predominantly within 2 km of the well (along Transects FP-0 and FP-1, and to a lesser extent along FP-2; Fig. S-1). Upon closer inspection it was determined that these white clusters actually were part of a near-continuous layer (deposit) that was mostly covered by a less dense and easily-disturbed, darker-colored flocculent layer (Fig. 5B). Samples of the white, star-like material protruding above the floc were "surgically" collected using the slurp gun at eight locations (Fig. S-1). GC/FID analysis of these confirmed that the white material contained nearly pure SBM-derived olefins (Fig. 6; see also Table S-3). Separate analyses of the overlying floc layer showed it to contain weathered oil derived from fallout of oil-laden marine snow from the deep sea plume (Stout and Payne, 2016; Stout et al., 2016). These seafloor observations (Fig. 5) and chemical analyses of these materials indicate that the SBM and oil-laden floc layers were deposited sequentially, whereupon the majority of the SBM was deposited shortly following the blowout and subsequent Top Kill operations, while deposition of the oil-laden floc continued to settle from the deep-sea plume during and for some time after the spill.

As noted above, a notable feature of the SBM-derived olefins found in some sediments is the presence of C_{11} to C_{14} *n*-alkanes (Fig. 4D). These *n*-alkanes were not observed in

any of the neat SBM's analyzed (Fig. 1), yet their abundance in some sediments, especially those containing a high concentration and proportion of TPH_{SBM} (Fig. 4D), and in the SBM-rich slurp gun filter samples (Fig. 6) is obvious. [The identity of these peaks as C_{11} to C_{14} *n*-alkanes was confirmed through full-scan GC/MS analysis in which molecular ions are consistent with *n*-alkanes rather than internal or branched olefins.] The origin of these *n*-alkanes is uncertain at present. There is no mechanism by which the C_{11} to C_{14} *n*-alkanes (only) would be preferentially preserved during the degradation of crude oil, and therefore their presence in sediments must be associated with SBM.

The absolute concentrations of SBM-derived olefins in sediments around the well in 2010/2011 are depicted in Fig. 7A, which shows the total concentration of C_{14}-C_{20} olefins (TPH_{SBM}) in the 118 olefin-containing sediments collected at different sediment depth intervals and distances from the well in 2010/2011. Summary statistics for the sediments collected from different depths in 2010/2011 are given in the top of Table 2. The highest concentrations of olefins were found in surface sediments (0-1 cm) between 0.5 and ~ 1.2 km from the well where the TPH_{SBM} concentrations mostly ranged between 1,000 and 10,000 μg/g (Fig. 7A). Overall, TPH_{SBM} concentrations were higher in surface sediments, where they averaged 3,270 μg/g, and generally decreased with increasing sediment depth (Table 2). The highest TPH_{SBM} concentration observed in any sediment was 28,654 μg/g, which occurred in a surface (0-1 cm) sediment 1 km northeast of the well that had contained nearly (96%) "pure" olefins – and the C_{11} to C_{14} *n*-alkanes discussed above (Fig. 4D). Overall, the TPH_{SBM} concentrations in sediments around the Macondo well are generally comparable to those previously-reported in sediments near wells that had been impacted by the conventional discharge of SBM-laden rock cuttings during normal drilling operations (CSA, 2004a,b). As noted above, however, the 6.5 km^2 "footprint" of the SBM-impacted sediments around the Macondo well (Fig. 3) is significantly larger than at conventional drill sites (< 250 m radius or 0.2 km^2; CSA, 2004a,b).

All 40 cores that had contained SBM-derived olefins at their surface (0-1 cm) also contained olefins within the 1-3 cm interval; i.e. the same "footprint" as shown in Fig. 3. Sediments collected from the 1-3 cm depth mostly contained between 100 and 1,000 μg/g TPH_{SBM} (Fig. 7A), and on average, contained only 431 μg/g TPH_{SBM}, i.e., about an order of magnitude lower than was found in surface (0-1 cm) sediments (Table 2).

However, a few cores contained a higher concentration of TPH_{SBM} in the 1-3 cm interval than was present at the core's surface (Fig. 7A) indicating deposition of SBM-derived olefins may have decreased over time at some locations or the SBM concentrations were diluted or buried by subsequently deposited oil-laden floc (see above).

Fewer cores contained deeper sediments (3-10 cm) impacted by SBM-derived olefins. Only 24 of the 40 cores collected from within the SBM "footprint" contained SBM-derived olefins in the 3-5 cm depth interval and 14 of these 24 also contained SBM-derived olefins in the 5-10 cm depth interval (Table 2). The concentration of TPH_{SBM} in both of these deeper sediments was generally between about 20 and 100 μg/g (Fig. 7A) and averaged only 50 μg/g (Table 2). The 14 cores containing olefins between 5 and 10 cm deep spanned the same approximate 2.6 km^2 "footprint" as represented by the surface sediments. Even the core collected at the southwestern-most extent of the SBM "footprint," located 2.3 km southwest of the well (Fig. 3), contained 50 μg/g of SBM-derived olefins below 5 cm depth (Fig. 7A; Table S-1). However, the occurrence of olefins in deeper sediments within the "footprint" was less contiguous indicating thicker deposition of SBM was more "patchy" within the impacted area. The concentrations of SBM-derived olefins in 3-10 cm deep sediments were markedly lower, however, with the maximum TPH_{SBM} concentration being only 104 μg/g (Fig. 7A; Table 2).

Although our study was not intended to address the impact of SBM deposition on benthic macrofauna, visual observations made from less than 1 m above the seafloor during the continuous transects near and southwest of the well (Fig. S-1) revealed marked differences in the abundance (and apparent health) of benthic organisms. For example, except for three isolated crabs encountered and photographed along FP-0 (Fig. S-3) there were few other visible signs of benthic macrofauna observed along transects FP-0 to FP-4 (Fig. S-1) in April 2011. Only further to the southwest, along FP-5 (Fig. S-1) were the diversity and frequency of benthic macrofauna observed to be comparable to observations made at greater distances from the wellhead (Fig. S-4). Although these observations are qualitative they nonetheless reflect an obvious and greater impact of SBM (and oil) deposition on benthic macrofauna nearer the well.

3.3 SBM in Deep-Sea Sediments in 2014

For the 830 sediments collected and analyzed in 2014, SBM-derived olefins were recognized within the GC-FID chromatograms of 74 sediments (~9%). An inventory of these is provided in Table S-2 of the *Supporting Materials*. Six of the 74 sediments containing SBM-derived olefins were from three cores collected 19, 52, and 62 km away from the well (Table S-2) and are not reasonably attributed to DWH incident, but rather to past drilling activities (see Section 3.5) Of the 68 samples containing SBM-derived olefins attributed to the DWH incident, all but one sample were collected within 1.8 km of the well within an approximately 6.5 km^2 "footprint;" the lone outlier was a surface sediment sample collected from a core 3.1 km to the northeast of the well (Fig. 8). Although configured slightly differently, perhaps owing to the fewer number of cores collected around the well in 2014, the 2010/2011 and 2014 SBM-derived olefin "footprints" were largely comparable (compare Figs. 3 and 8). Thus, the persistence of the SBM-derived olefin "footprint" in sediments around the Macondo well in the four years that had passed since the DWH incident was confirmed.

However, the concentrations of TPH_{SBM} in the sediments collected in 2014 were generally lower than had been observed in 2010/2011 (Fig. 7B; Table 2). For example, the 23 surface sediments within the SBM-derived olefin footprint in 2014 contained, on average, only 372 μg/g, which is an order of magnitude lower than was observed in 2010/2011 (Table 2). Conversely, the concentrations of olefins in deeper sediment intervals (1-3, 3-5 and 5-10 cm) in 2014 were more comparable to those observed in 2010/2011. Although fewer samples were collected in 2014 these results suggest that the concentration of SBM-derived olefins in surface (0-1 cm) sediments may have been preferentially reduced (relative to those in deeper sediments) over the four years since the DWH incident. Multiple mechanisms for the reduction in surface sediment concentrations are possible, including microbial biodegradation and physical processes such as resuspension, bed transport, burial by natural sediment deposition, and/or mixing (bioturbation). The former undoubtedly contributed given the chemical changes in the character of the SBM-derived olefins (and the co-occurring oil) consistent with biodegradation (Section 3.4; discussed below).

Fig. 9 shows GC-FID chromatograms for four SBM-impacted sediments collected in 2014. As was evident among the 2010/2011 samples, the proportions of SBM-derived olefins and crude oil present in sediments varied widely. Some sediments contained

predominantly weathered oil with only traces of SBM-derived olefins (Fig. 9A-B) while others contained nearly "pure" SBM (Fig. 9D). The %TPH as TPH_{SBM} for all samples ranged from 3 to 98% (Table S-2). This indicates that as little as 3% of the TPH could still be recognized as C_{14} to C_{20} SBM-derived olefins, which were not "lost" into the UCM hump of the weathered oil.

In contrast to the 2010/2011 results, crude oil was consistently weathered in the sediments collected in 2014. Specifically, most oil-impacted sediments with 1.6 km of the well collected in 2010/2011 exhibited a broad UCM extending up to around C_{40} with prominent *n*-alkanes spanning this range (Fig. 4A-B; Stout and Payne, 2016). This oil was relatively unweathered, and the lack of weathering was attributed to its more direct deposition of particulate oil around the well during the blowout perhaps facilitated by an association with SBM (Stout and Payne, 2016). However, by 2014 the oil residues in these proximal (<1.6 km) sediments are severely weathered, as indicated by a UCM that gradually rises between about C_{10} and C_{25} and retention of only the more recalcitrant *n*-C_{25}+ *n*-alkanes (Fig. 9A-C). Stout and Payne (2016) had observed similarly weathered Macondo oil in surface sediments collected further from the well (~1.6 to 8 km) in 2010/2011. Owing to the increased degree of weathering of the oil with increasing distance from the well, these researchers attributed the oil's distinct high boiling, wax-enriched character to severe dissolution and biodegradation during its lateral transport as dispersed oil droplets within the deep-sea plume and prior to its deposition on the seafloor. The comparably weathered character of the oil residues found in sediments collected less than 1.6 km from the well in 2014 (Fig. 9) indicates that between 2010/2011 and 2014, biodegradation of the oil originally deposited in these sediments had progressed (Fig. 9). In turn, biodegradation of the SBM-derived olefins is also anticipated – and is discussed in Section 3.4.

3.4 Biodegradation of SBM-derived Olefins in Sediments

Numerous microcosm and seafloor studies have demonstrated the biodegradability of SBM-derived olefins as measured through respiration rates (e.g., CO_2 generation) or total TPH mass loss (OGP, 2003; Neff et al., 2000). Previous studies have not (to our knowledge) addressed the molecular effects of microbial biodegradation on olefin isomer patterns, which our data permit, at least qualitatively. The presence of SBM-derived olefin clusters in impacted sediments from 2010/2011 and 2014 was clearly

visible in conventional GC-FID chromatograms of the sediments (Figs. 4 and 9). This made its presence and TPH_{SBM} concentration relatively easy to recognize and quantify. There was an overall (approximate order of magnitude) reduction in TPH_{SBM} concentration between 2010/2011 and 2014 (Fig. 7; Table 2), although this reduction cannot be assumed to be entirely due to biodegradation (as opposed to bioturbation or sediment redistribution). However, biodegradation had clearly occurred. Multiple studies following the DWH disaster demonstrated the presence of an indigenous and diverse microbial community in surface sediments near the wellhead, including species capable of olefin-degradation (Mason et al., 2014; Kimes et al., 2014). In addition, detailed characterization of the isomer pattern(s) within each olefin cluster, revealed an overall change in the molecular character of the olefins that is only reasonably attributable to microbial biodegradation, as described herein.

All of the neat SBMs studied had exhibited generally comparable patterns in that the C_{16} olefin clusters predominated over the C_{18} cluster, which in turn predominated over the C_{15} and C_{17} clusters (Table 2; Fig. 1). Another common feature among the neat SBMs studied was a prominence of the LAO and multiple IO isomers within all of the clusters (see α and peaks a, b, and c in Figs. 2 and S-2). In addition, within the C_{16} and C_{18} olefin clusters only there were a series of early-eluting peaks considered, based upon the hydrogenation results of Aeppli et al. (2013), to be numerous MBO isomers (Section 3.1). These C_{16} and C_{18} MBOs were present in much lower proportions than the corresponding LAO and IOs in the neat SBMs (Figs. 2 and S-2).

In our review of the SBM-derived olefin “fingerprints” observed in the sediments collected in 2014 it became evident that two changes between or within the isomer cluster were regularly observed, *viz*. (1) the relative abundance of C_{16} olefins was reduced relative to C_{18} olefins and (2) the relative abundance of C_{16} and C_{18} LAOs and IOs were reduced relative to C_{16} and C_{18} MBOs. These changes were (in part) evident in Fig. 9, wherein the dominance of the C_{16} olefins, such as was evident in the neat SBMs (Fig. 1) and 2010/2011 sediments (Fig. 4), often had been reduced relative to the other olefin clusters within the 2014 sediments (Fig. 9A-B and D). The progression in weathering, however, is more clearly demonstrated in the three SBM-impacted sediments from 2014 shown in Fig. 10, which compares the detailed distributions of olefins within three 2014 sediments.

Some sediments collected in 2014 contained minimally weathered SBM-derived olefins whose distribution between and within the olefin clusters (Fig. 10A) was largely consistent with the "fresh" neat SBM (Fig. 2). However, other sediments were observed to have reduced proportions of C_{16} olefins relative to C_{18} olefins and reduced LAO and IO (peak α and peaks a, b, and c, respectively) C_{16} and C_{18} isomers relative to corresponding MBOs (Fig. 10B-C). (It is notable that the methyl-branched olefin peak arbitrarily labelled as "b" herein is actually represented by two peaks, which can be seen in Fig. 10C). The observed preferential loss of the C_{16} olefins relative to the C_{18} olefins could derive from the former's expectedly higher aqueous solubilities and resultant bioavailability to microbes, which perhaps facilitated their partitioning into seawater and/or biodegradation over time. (Evaporation, of course, should play no role in weathering in the deep-sea.) However, the reduction in C_{16} and C_{18} LAO and IO isomers relative to MBO isomers cannot be explained by any abiotic process and must be due to biodegradation.

Branched hydrocarbons are generally less susceptible to biodegradation compared to straight-chain hydrocarbons, and susceptibility further decreases with the degree of branching (Atlas, 1995). For the SBM-derived olefins it appears that the presence of (at least) a single methyl-branch is sufficient to retard the rate of biodegradation of the C_{16} and C_{18} MBOs relative to the corresponding LAOs and IOs in sediment (Fig. 10). The LAO within the C_{16} and C_{18} clusters appear to be reduced to the approximate same degree as the corresponding IOs. Additionally, the relative proportions among the prominent IO isomers (peaks a, b, and c) are largely maintained. This apparent comparable susceptibility among LAO and IO isomers suggests that the position of the double-bond (α- *versus* multiple internal positions) does not seem to affect the susceptibility of these linear olefins to biodegradation.

The biodegradation of the LAO and IOs evident in the 2014 sediments (Fig. 10) may have commenced sooner, even within some 2010/2011 sediments. However, the co-occurrence of less weathered crude oil in these 2010/2011 sediments reduced our ability to recognize and monitor the detailed changes within the C_{16} and C_{18} olefin isomer abundances or patterns due to prominent and co-eluting crude oil-derived hydrocarbons (Fig. 4). However, by 2014, 4 years after the SBM was released, and after the crude oil

had sufficiently weathered (and co-eluting oil-derived hydrocarbons were themselves biodegraded) the change in olefin cluster abundance and individual isomer patterns was more evident (Figs. 9 and 10). Notably, none of the SBM-impacted sediments collected in 2014 contained any of the C_{18} to C_{24} FAMEs present in some of the neat SBMs (starred peaks in Fig. 1B-C) and that had been rarely observed in sediments collected in 2010/2011 (Fig. 4C). Their absence from all sediments collected in 2014 suggests these FAMEs were completely dissolved and/or biodegraded.

Although it was beyond the scope of our study, future studies involving SBM-derived olefins in sediments may attempt to exploit the greater susceptibilities of LAOs and IOs to biodegradation (*versus* MBOs) to quantity biodegradation of SBM-derived residues of SBMs containing these olefin groups in sediments. For example, based upon the results observed herein, the ratio of (LAO+IO)/MBO should decrease with increased weathering within the C_{16} and C_{18} olefin clusters.

Finally, based upon the variation in the degree of biodegradation apparent in over the 4-year time period represented by the 2014 sediments studied (e.g., Fig. 10A-C) it is clear that factors other than time (e.g., olefin and oil concentrations, oxygen availability, etc.) collectively will determine the rates at which SBM-derived olefins will biodegraded in the deep-sea sediments around the Macondo well.

3.5 Persistence of SBM-derived Olefins at Former Drill Sites

As noted in Sections 3.2 and 3.3, in both 2010/2011 and 2014 numerous sediment samples (25 and 6, respectively; Tables S-1 and S-2) collected at varying distances from the Macondo well were recognized to contain SBM-derived olefins that were not reasonably attributable to the DWH incident. Most of these were located 20 to 62 km from the Macondo well, including 16 sediments from four proximal cores collected in both 2011 and 2014 located 62 km northeast of the Macondo well (i.e., in Viosca Knoll Block 916 area, not shown on Figs. 3 and 8; see Fig. S-5). Each of these four cores contained SBM-derived C_{15} to C_{19} olefin clusters in surface (0-1 cm) and each subsurface sediment interval studied up to 10 cm deep. The GC-FID chromatograms for each sediment interval through one of these cores are shown in Fig. 11.

Each sediment throughout the core contained prominent olefins dominated by the C_{16} and C_{18} clusters containing LAO, IO, and MBO isomers – and in this regard generally resembled the type of SBM released during the DWH incident. No oil is recognized in these sediments suggesting they were impacted only by SBM. The concentration of TPH_{SBM} in these 16 sediments ranged from 7 to 1,219 μg/g and averaged 247 ± 369 μg/g. (± 1σ; Table S-1). These TPH_{SBM} concentrations are generally comparable to most sediments collected near the Macondo well (Fig. 7; Table 2). Given their distance from the Macondo well, however, the SBM-derived olefins cannot reasonably be attributed to the DWH incident – but rather to conventional discharges of SBM at a former drill site(s) in the Viosca Knoll Block 916 area. A review of the BOEMRE well site database (https://www.data.boem.gov/ homepg/data_center/well/well.asp) shows all these four cores were located within 50 m of an oil exploration well that had completed drilling in November 2001 (Well ID: 608164037600). No other (particularly any more recent) exploration or production wells are located in the area of these cores. Thus, the presence of SBM-derived olefins in multiple cores and sediments up to 10 cm deep indicates these chemicals were discharged in the area in 2001 (when drilling ceased) and had persisted in these deep-sea sediments up to 13 years.

The detailed distributions among SBM-derived olefins in these sediments exhibit evidence of preferential weathering (biodegradation) of (1) the C_{16} over C_{18} olefins (Fig. 11A-D) and (2) C_{16} and C_{18} LAO and IO isomers over MBOs (Fig. 11E), both of which were also observed to have occurred in sediments near the Macondo well (Fig. 10). The comparable biodegradation effects on the mixed (LAO/IO/MBO) olefin-based SBMs at the Macondo and Viosca Knoll Block 916 wells speaks to the consistent manner by which Gulf of Mexico seafloor microbes attacked the SBMs discharged at the two sites. It is notable that even after 10 or more years the most biodegraded SBM-derived olefin residues found in the Viosca Knoll Block 916 area well's sediments are not significantly different than the residues present near the Macondo well four years after discharge (compare Figs. 10C and 11E). In both instances residues of C_{15} to C_{18} olefins persist – they are not entirely removed by biodegradation. Thus, although specific seafloor conditions (e.g., temperature, oxygen or other electron acceptor availability, grain size, etc.) may vary, one might anticipate that the SBM-derived olefins and olefin "footprint" near the failed Macondo well (Figs. 3 and 8) will persist for (at least) a comparable duration.

4. Conclusions

Synthetic-based drilling mud (SBM) was discharged into the Gulf of Mexico during the drilling of the Macondo well, the *Deepwater Horizon* (DWH) blowout, and failed "Top Kill" operation in 2010. Representative neat SBMs consisted predominantly (86 and 93 wt%) of olefins within the C_{14} to C_{20} range (TPH_{SBM}) and minor C_{13} olefins and C_{18} to C_{24} even-carbon-number fatty acid methyl esters (FAMEs). Each olefin cluster was comprised of mixtures of the corresponding linear α-olefin (LAO) and numerous internal olefin (IO) isomers while the C_{16} and C_{18} (and perhaps C_{20}) clusters only also included numerous mostly methyl-branched (MB) isomers. The distinctive chromatographic appearance of SBM made its presence easy to recognize and quantify in deep-sea sediments collected following the DWH disaster.

In 2010/2011 (4 to 18 months after the blowout), 143 sediments (~5% of the 2,782 samples) were determined to contain SBM-derived olefins. Most of these sediments (118) were obtained from multiple sediment depth intervals (0-1, 1-3, 3-5, and 5-10 cm) from 40 cores collected within 2.3 km of the failed Macondo well within an SBM "footprint" covering approximately 6.5 km^2 of the seafloor around the Macondo well. Nearly all of the 2010/2011 sediments that contained SBM-derived olefins also contain some spilled Macondo oil, but the proportions of each (SBM and oil) varied widely, which indicates the oil and SBM-derived olefins did not "travel together" to reach the seafloor.

The highest concentrations of SBM-derived olefins were found in surface sediments (0-1 cm) between 0.5 and ~1.2 km from the well where the TPH_{SBM} concentrations mostly ranged between 1,000 and 10,000 μg/g (avg. 3,270 μg/g), and generally decreased with increasing sediment depth. The highest TPH_{SBM} concentration observed in any sediment was 28,654 μg/g, which occurred in a surface (0-1 cm) sediment 1 km northeast of well. The occurrence of olefins in subsurface sediments (1-10 cm) was less contiguous than in surface sediments indicating thicker deposition of SBM was more "patchy" within the impacted area. Overall, the TPH_{SBM} concentrations in sediments around the Macondo well are generally comparable to those previously-reported in sediments near wells that had been impacted by the conventional discharge of SBM-laden rock cuttings during normal drilling operations. However, the ~6.5 km^2

"footprint" of the SBM-impacted sediments around the Macondo well is significantly larger than is typical at conventional drill sites (<0.2 km^2).

In 2014, approximately 4 years after the DWH disaster, 68 of the 830 sediment samples studied contained SBM-derived olefins attributed to the incident. All but one of these were from 23 cores collected within 1.8 km of the well and within an approximately 6.5 km^2 "footprint" akin to that observed in 2010/2011, which demonstrated the persistence of the SBM-derived olefin "footprint" in sediments around the Macondo well. However, the TPH_{SBM} concentration in surface sediments collected in 2014 mostly range from 10 to 1,000 μg/g (avg. 372 μg/g), which is an order of magnitude lower than levels observed in 2010/2011. As in 2010/2011 the SBM-derived olefins co-occurred with varying amounts of Macondo crude oil, the latter of which appeared severely biodegraded compared to 2010/2011.

The SBM-derived olefins in sediments collected 4 years after the DWH incident also were biodegraded, but to varying degrees, which undoubtedly contributed to the reduced TPH_{SBM} concentrations (perhaps aided by physical processes such as resuspension, bed transport, burial by natural sediment deposition, and/or bioturbation). Biodegradation of the SBM-derived olefins was revealed by (1) a reduction in the abundance of (the originally dominant) C_{16} olefins relative to C_{18} olefins and (2) a reduction in the relative abundance of C_{16} and C_{18} LAOs and IOs relative to C_{16} and C_{18} MBOs. Both LAO and IO isomers appear equally susceptible to biodegradation indicating the position of the double bond does not seem to affect the susceptibility. The FAMEs present in some of the neat SBMs were rarely observed in sediments collected in 2010/2011 and absent from all sediments collected in 2014, suggesting these esters were completely dissolved and/or biodegraded – and were thereby more susceptible to weathering than the olefins.

Based upon the variation in the degree of biodegradation in SBM-derived olefins among the 2014 sediments studied it is clear that factors other than time (e.g., olefin and oil concentrations, oxygen availability, etc.) affect the rates at which SBM-derived olefins will biodegraded in the deep-sea sediments around the Macondo well.

Our 2010/2011 and 2014 assessments of the seafloor encountered SBM-derived olefins in sediments also show deposits attributable to the conventional discharge of SBM-laden cuttings at former drill sites. In the Viosca Knoll/Block 916 area (62 km northeast of Macondo) and within 50 m of an oil exploration well that had completed drilling in 2001, 16 sediments up to 10 cm deep contained 7 to 1,219 μg/g TPH_{SBM} (avg. 247), which indicates SBM-derived olefins had persisted in these deep-sea sediments up to 13 years. Although specific seafloor conditions (e.g., temperature, oxygen or other electron acceptor availability, grain size, etc.) may vary, one might anticipate that the SBM-derived olefins and the olefin "footprint" near the failed Macondo well will persist for (at least) a comparable duration.

Acknowledgments

The authors wish to thank the efforts of numerous Trustee and BP field teams that cooperatively planned and collected the deep-sea samples used in this analysis, an effort unprecedented in oil spill investigations. The efforts of Christopher Lewis (Industrial Economics, Corp.), Robert Ricker (NOAA), and Debbie French-McCay (RPS-ASA) in organizing the sample collection efforts are specifically acknowledged. The authors also wish to thank Greg Baker (NOAA), Nancy Rothman (New Horizons), William B. Driskell (Driskell Consultants), Ann Jones (Industrial Economics, Corp.) for coordinating the large analytical program. The efforts of numerous NewFields staff who aided in the management of the chemical analyses (Wendy Wong and Eric Litman), database (George Desreuisseau and Gang Hu), and GIS (Bo Liu) are also acknowledged.

Disclosure

This study was conducted within the *Deepwater Horizon* NRDA investigation, which was cooperatively conducted by NOAA, other Federal and State Trustees, and BP. The scientific results and conclusion of this publication, as well as any views or opinions expressed herein, are those of the authors and do not necessarily represent the view of NOAA or any other natural resource Trustee for the BP/Deepwater Horizon NRDA. The authors declare no competing financial interest in the publication of this study. Funding for the study was provided by NOAA as part of the NRDA process.

References

Aeppli, C., Reddy, C.M., Nelson, Kellerman, M.Y., Valentine, D.L. 2013. Recurrent oil sheens at the *Deepwater Horizon* disaster site fingerprinted with synthetic hydrocarbon drilling fluids. Environ. Sci. Technol. 47(15), 8211-8219.

Atlas, R.M., 1995. Petroleum biodegradation and oil spill bioremediation. Mar. Pollut. Bull. 31, 178-192.

British Petroleum. 2010. BP/Deepwater Horizon Rheliant Displacement Procedure OSC-G-32306 (MiSWACO); obtained from BP Deepwater Horizon– MDL 2179 Trial Docs – Phase 1 Trial; access on Web at: http://www.mdl2179trialdocs.com/releases/release201304041200022/TREX-00567.pdf

Camilli, R., Reddy, C.M., Yoerger, D.R., Van Mooy, B.A.S., Jakuba, V.M., Kinsey, J.C., McIntyre, C.P., Sylva, S.P., Maloney, V.M. 2010. Tracking Hydrocarbon Plume Transport and Biodegradation at *Deepwater Horizon*. Science 330, 201-204.

Continental Shelf Associates, 2004a. Gulf of Mexico comprehensive synthetic based muds monitoring program. Final Report, Volume 1: Technical. Prepared for Synthetic Based Muds Research Group, Oct. 2004. http://www.boem.gov/Environmental-Stewardship/Environmental-Studies/Gulf-of-Mexico-Region/GOMR-Environmental-Reports-Index.aspx

Continental Shelf Associates, 2004b. Gulf of Mexico comprehensive synthetic based muds monitoring program. Final Report, Volume 2: Technical. Prepared for Synthetic Based Muds Research Group, Oct. 2004. http://www.boem.gov/Environmental-Stewardship/Environmental-Studies/Gulf-of-Mexico-Region/GOMR-Environmental-Reports-Index.aspx

Curiale, J.A. and Frolov, E.B. 1988. Occurrence and origin of olefins in crude oils. A critical review. Org. Geochem. 29(1-3), 397-408.

Department of Energy, 2014. http://energy.gov/downloads/microsoft-powerpoint-53-item-01-top-kill-operation-status-09-june-1400pptx.

Kimes, N.E., Callaghan, A.V., Suflita, J.M., Morris, P.J. 2014. Microbial transformation of the Deepwater Horizon oil spill – past, present, and future perspectives. Frontiers Microbiol. 5: 1-11.

Mason, O.U., Scott, N.M., Gonzalez, A., Robbins-Pianka, A., Baelum, J., Kimbrel, J., Bouskill, N.J., Prestat, E., Borglin, S., Joyner, D.C., Fortney, J.L., Jurelevicius, D., Stringfellow, W.T., Alvarez-Cohen, L., Hazen, T.C., Knight, R., Gilbert, J.A., Jansson, J.K. 2014. Metagenomics reveals sediment microbial community response to Deepwater Horizon oil spill. ISME J. 8: 1464-1475.

MiSWACO, 2010. BP Maconda (*sic*). Technical services laboratory report, ID Code No. 100513F.001, Lab Master No. 20101479. May 13, 2010. 3 p.

Neff, J. M., McKelvie, S., Ayers, R.C. Jr., 2000. Environmental impact of synthetic based drilling fluids. U.S. Dept. of the Interior, Minerals Management Service, Gulf of Mexico OCS Study MMS 2000-064. www.data.boem.gov/PI/PDFImages/ *ESPIS/3/3175.pdf.*

NOAA, 2014. Analytical quality assurance plan, Mississippi Canyon 252 (*Deepwater Horizon*) natural resource damage assessment, Version 4.0. May 30, 2014.

Oil and Gas Producers, 2003. Environmental aspects of the use and disposal of non-aqueous drilling fluids associated with offshore oil and gas operations. Int'l. Assoc of Oil and Gas Producers, Report No. 342, May 2003, 65 p.

Payne, J.R. and W.B. Driskell. 2015. *Deepwater Horizon* oil spill NRDA offshore adaptive sampling strategies and field observations. PECI Technical Report to the Trustees in support of the PDARP. (www.doi.gov/deepwaterhorizon/admin record, DWH-AR0023786, 75 pp.).

Reddy, C.M., Nelson, R.K., Sylva, S., Xu, L., Peacock, E.A., Raghuraman, B., Mullins, O.C., 2007. Identification and quantification of alkene-based drilling fluids in crude oils by comprehensive two-dimensional gas chromatography with flame ionization detection. J. Chromatogr. A, 1148(1), 100-107.

Socolofsky, S.A., Adams, E.E., and Sherwood, C.R., 2011. Formation dynamics of subsurface hydrocarbon intrusions following the Deepwater Horizon blowout. *Geophys. Res. Lett.* 38: L09602.

Spaulding, M.S., Mendelsohnm, D, Crowley, D., Li, Z., and Bird, A. 2015 Technical Reports for Deepwater Horizon Water Column Injury Assessment—WC_TR 13. Application of OILMAP DEEP to the Deepwater Horizon Blowout. RPS ASA, 55 Village Square Drive, South Kingstown, RI 02879. August 2015.

Stout, S.A. and Payne, J.R. 2016. Macondo oil in deep-sea sediments: Part 1 – sub-sea weathering of oil deposited on the seafloor. Mar. Pollut. Bull., 111(1-2): 365-380.

Stout, S.A., Payne, J.R., Ricker, R.W., Baker, G., Lewis, C. 2016. Macondo Oil in Deep-Sea Sediments, Part 2 – Distribution and distinction from background and natural oil seeps. Mar. Pollut. Bull., 111(1-2): 381-401.

Table 1: Neat synthetic based mud samples analyzed and selected results.

Sample	Vessel	Collection Date	Collection Time (CST)	TPH (ug/g)	TPH_{SBM} (ug/g)	%TPH as C_{14}-C_{20} Olefins	Percent Olefins by Carbon Number						
							C14	C15	C16	C17	C18	C19	C20
GU2909-A0602-OTARF2519	Carol Chouest[4]	06/02/10	19:11	<47,700	na	na	ndp	ndp	ndp	ndp	ndp	ndp	ndp
GU2909-A0602-OTARF2527	Carol Chouest[5]	06/02/10	19:37	<41,300	na	na	0	16	33	13	35	2	1
GU2909-A0602-OTARF2501	Infant Jesus[1]	06/02/10	15:37	64,800	33,900	52	4	11	38	11	33	2	2
GU2909-A0602-OTARF2511	Kylie Williams[3]	06/02/10	17:10	401,000	369,000	92	1	14	41	15	26	3	1
GU2909-A0602-OTARF2505B	Infant Jesus[2]	06/02/10	16:10	540,000	463,000	86	1	8	47	9	32	2	1
LAAR38-A0626-DMA801	HOS Centerline[6]	06/26/10	13:48	990,000	919,000	93	1	13	46	7	31	2	1
						Average:	1	12	41	11	31	2	1
						St. Dev.:	2	3	6	3	3	0.4	0.4

[1]rear tank, stirred 30 min every 4 hrs, sampled ~3' deep; [2] front tanks composite, stirred 30 min every 4 hrs, sampled ~3' deep; [3] equal mix of two tanks, tanks stirred 30 min every 6 hrs; [4] equal mix of two left side port tanks, stirred 30 min every 6 hr, sampled ~20' deep; [5] equal mix of two right side port tanks, stirred 30 min every 6 hrs, sampled 20' deep; [6] *Encore* mud (Halliburton), 4 hr stir.

Table 2: Statistics for the concentration (μg/g) of TPH_{SBM} in sediments containing SBM-derived olefins within the SBM "footprint" by year and depth. Calculated from data contained in Tables S-1 (2010/2011) and S-2 (2014). na-not available

2010/2011

Depth	0-1 cm	1-3 cm	3-5 cm	5-10 cm	10-15 cm
count	40	40	24	14	na
median	1362	148	44	49	na
mean	3270	431	50	50	na
max	28654	4066	98	104	na
min	14	22	20	20	na
stdev	5409	705	22	20	na

2014

Depth	0-1 cm	1-3 cm	3-5 cm	5-10 cm	10-15 cm
count	23	20	15	7	3
median	59	175	109	42	30
mean	372	534	292	48	49
max	3826	2641	1138	98	91
min	6	5	2	10	25
stdev	795	717	373	37	37

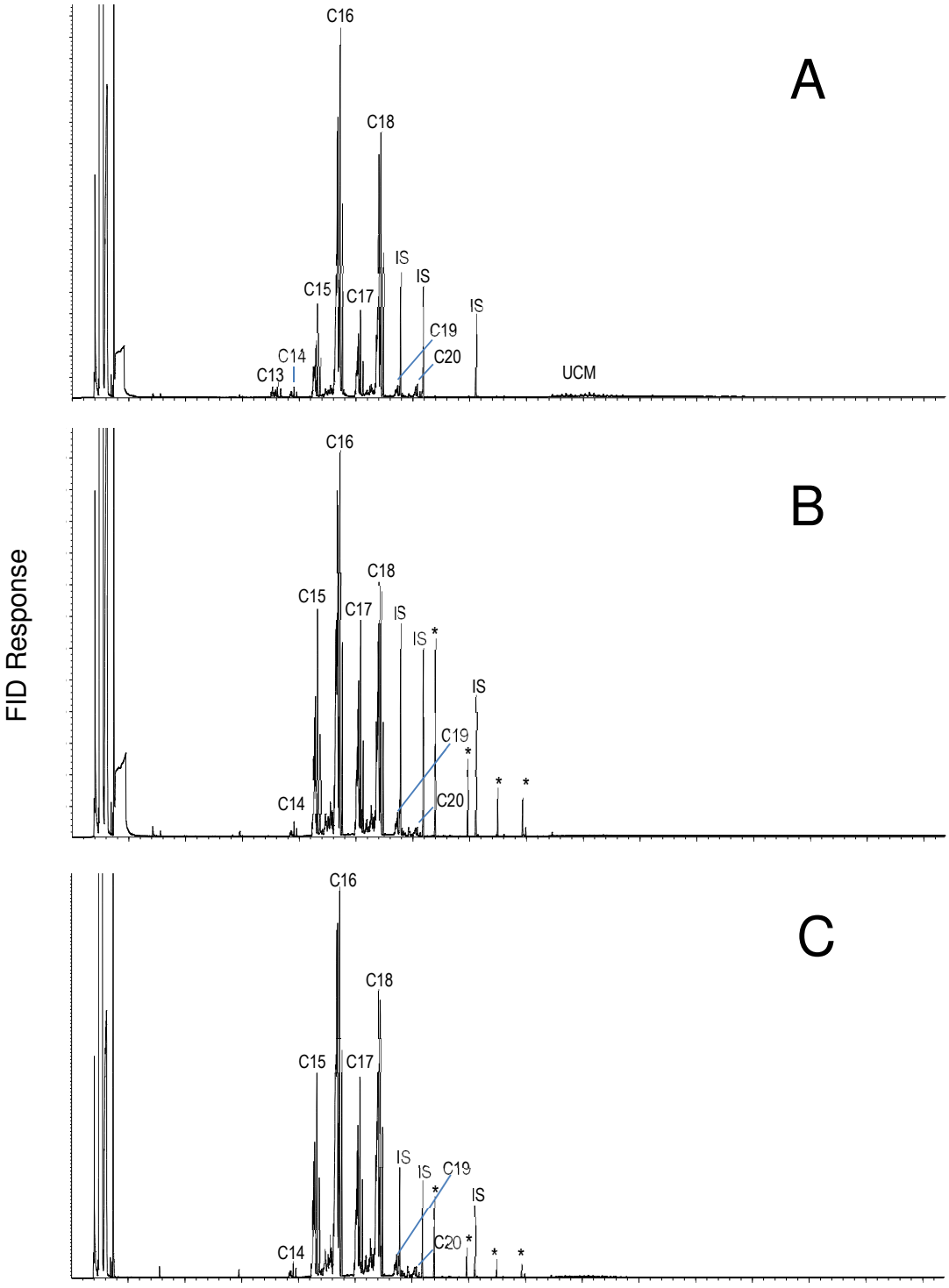

Figure 1: GC-FID chromatograms of extractable hydrocarbons in three synthetic based muds, (A) *Infant Jesus:* GU2909-A0602-OTARF2505B, (B) *Kylie Williams:* GU2909-A0602-OTARF2511, and (C) *HOS Centerline:* LAAR38-A0626-DMA801. C# - olefin cluster carbon number; IS – internal standard: * - (left to right) C_{18}, C_{20}, C_{22}, and C_{24} FAMEs. The large peak to the far left in each is laboratory solvent.

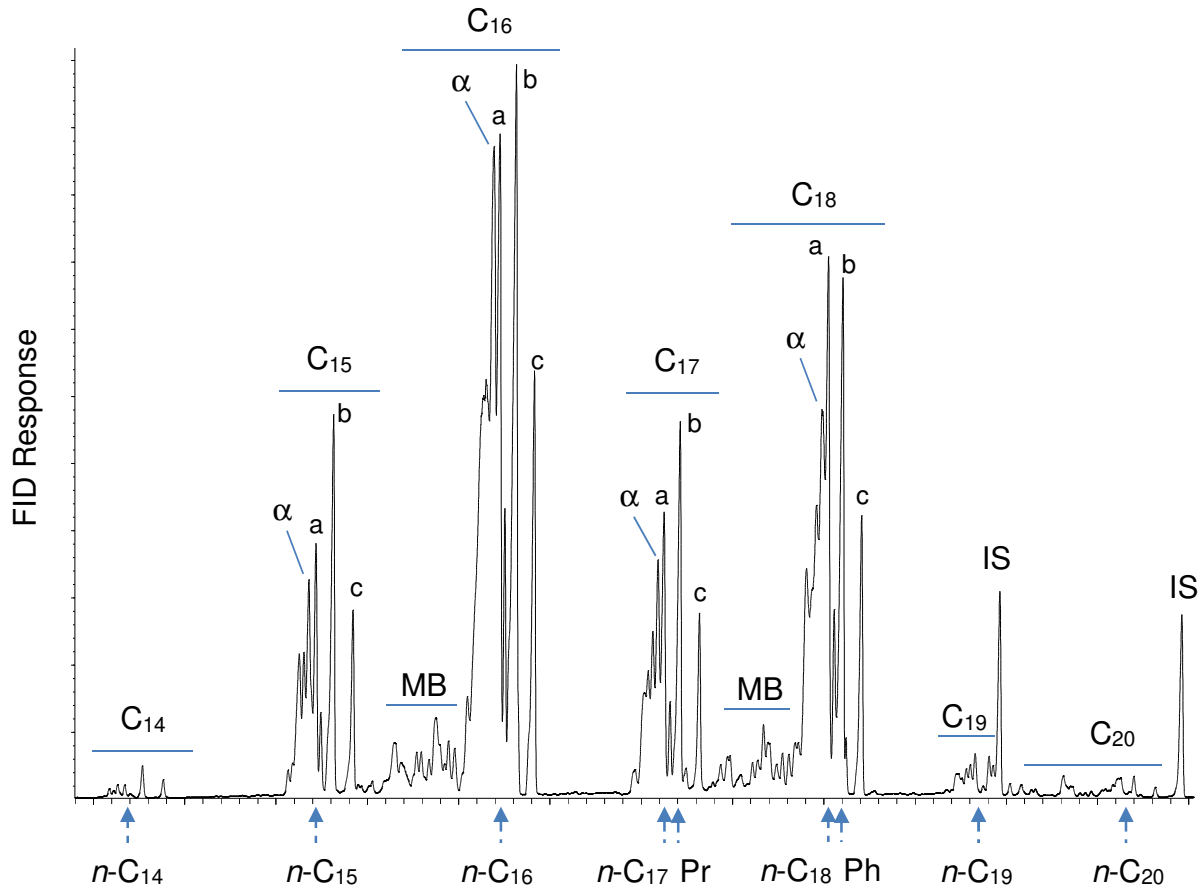

Figure 2: Partial GC-FID chromatogram of SBM from the *HOS Centerline* showing the olefin clusters between C_{14} and C_{20}. α: alpha olefins, MB: methyl-branched olefins, and a, b, and c: prominent internal olefin isomers (unidentified) only associated with C_{16} and C_{18} (and perhaps C_{20}) olefins. IS-internal standard. Arrows along bottom indicate elution time for *n*-alkanes, pristane (Pr) and phytane (Ph), which are absent in the SBM

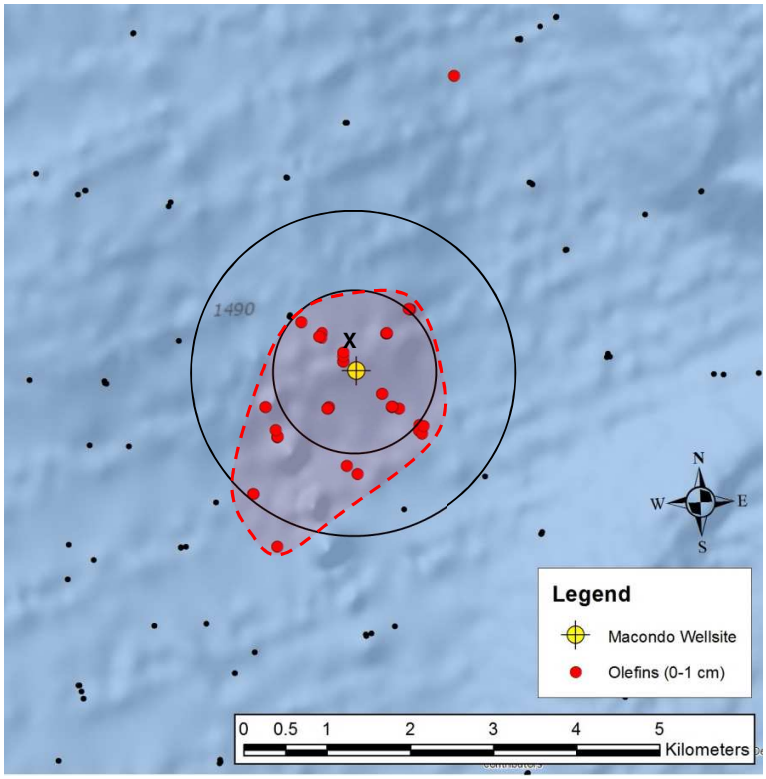

Figure 3: Map showing the cores collected in 2010/2011 showing those containing SBM-derived olefins within an approximate 6.5 km^2 "footprint" of SBM-impacted sediments around the Macondo well. Black dots show all core locations with no olefins present. Concentric circles depict 1 and 2 km radii from the well. "X" depicts the location of the sunken DWH rig approximately 0.5 km NNW of the well. . See Table S-1 for an inventory of all 2010/2011 sediment intervals containing SBM-derived olefins.

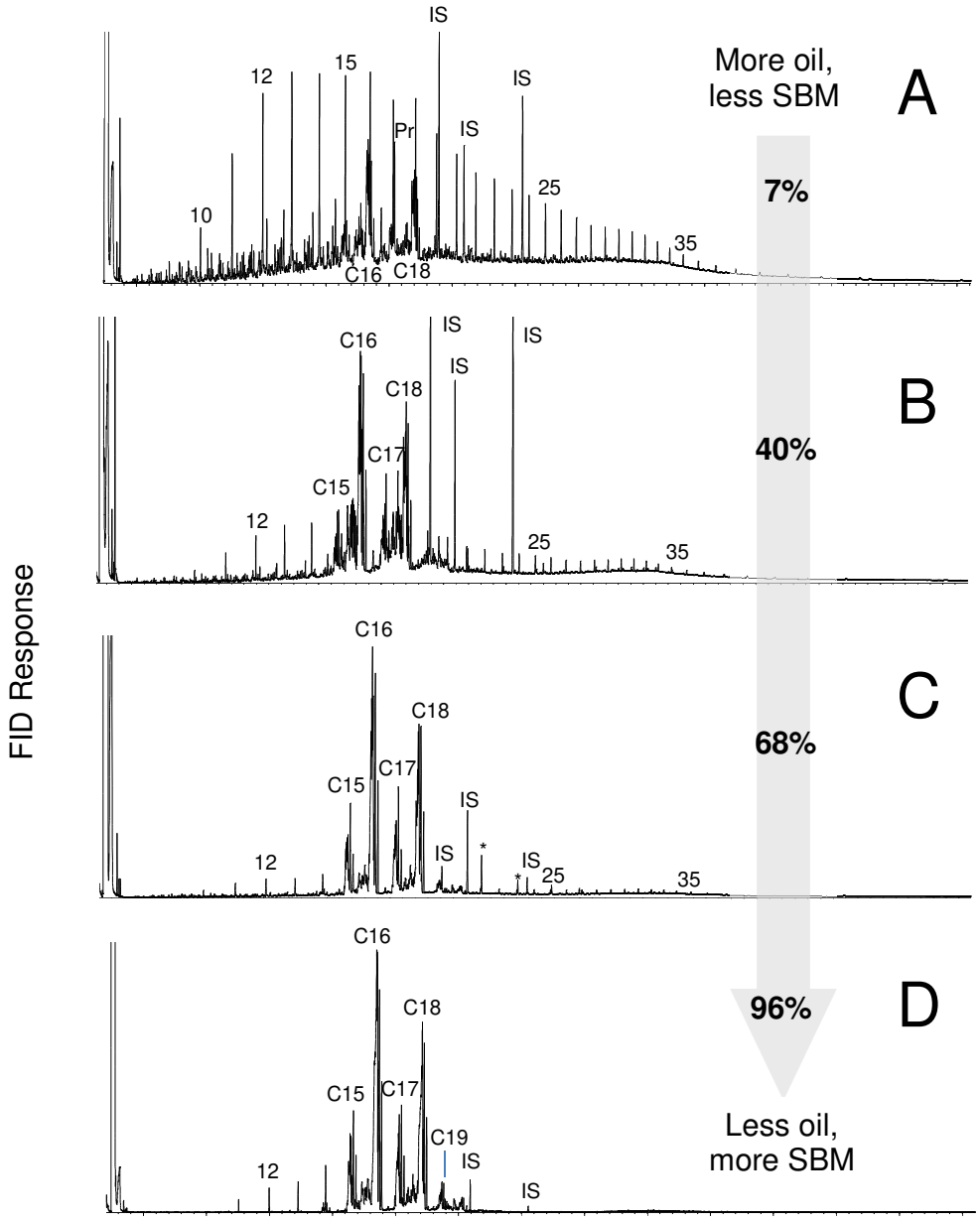

Figure 4: GC-FID chromatograms showing deep-sea surface (0-1 cm) sediments containing varying proportions of Macondo oil and olefin-based SBM. The %TPH as TPH_{SBM} in each is indicated along the arrow (per Table S-1). (A) SB9—65-B0528-S-D034S-HC-0969, (B) SB9-65-B0528-S-ALTNF001-HC-1207, (C) HSW2L2_ FP0094_B0423_S_50_H2_868, and (D) SB9-65-B0526-S-NF006MOD-HC-0379. #-*n*-alkane carbon number, Pr-pristane, C#-olefin cluster, IS-internal standard, * - C_{18} and C_{20} FAMEs. Apparent C_{11} to C_{14} *n*-alkanes in (B) to (D) are discussed in the text.

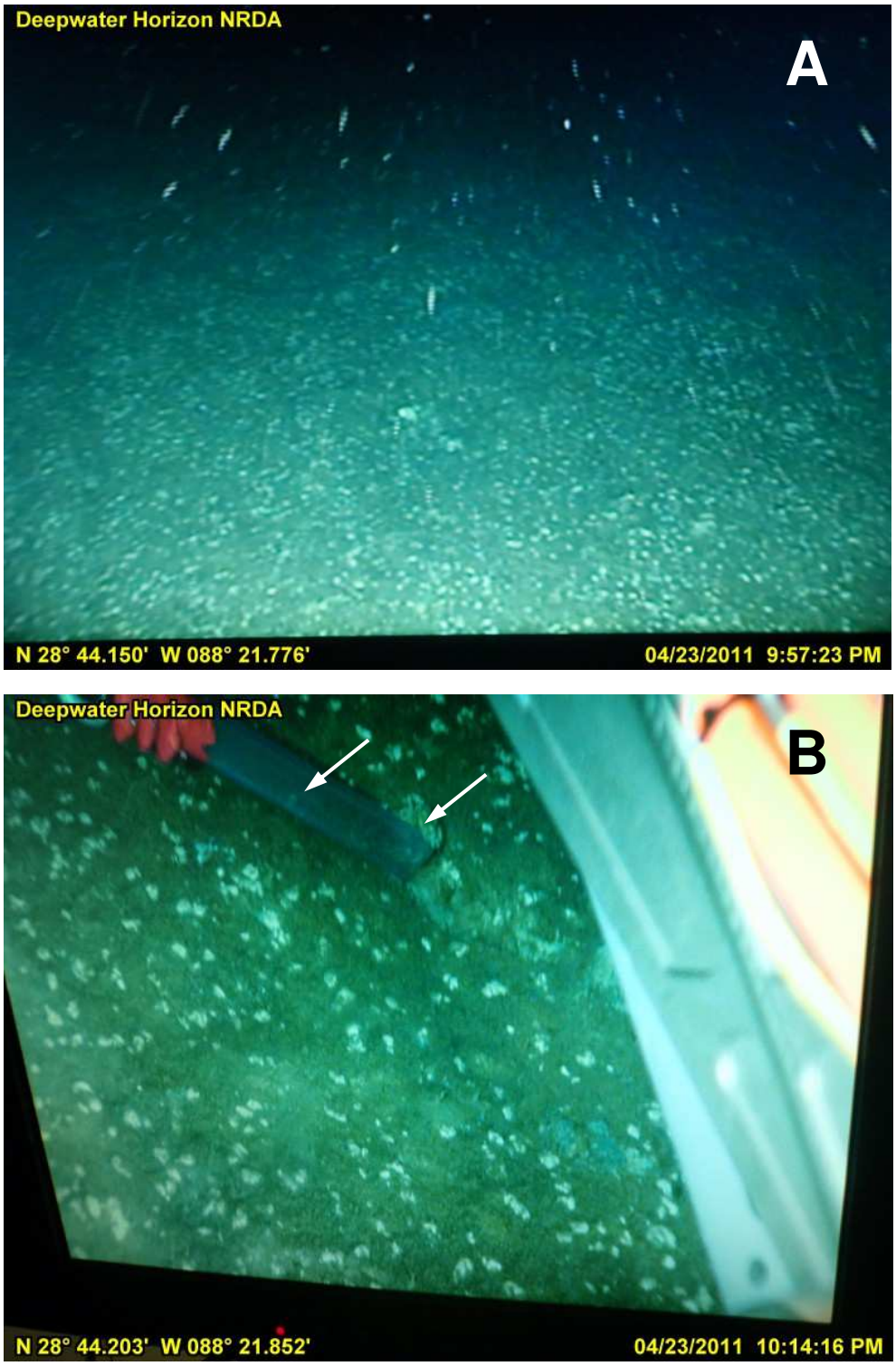

Fig. 5. Photographs of the seafloor impacted by SBM. (A) representative photograph of ubiquitous SBM coverage manifest as white "stars" protruding from a subsequently deposited layer of flocculent material observed along transects FP-0 and FP-1 (Fig. S-1) and (B) close-up showing slurp gun nozzle being used to vacuum white material (arrows). This photo shows collection of a nearly pure SBM sample (HSW2L2_FP0094_B0423_W_ 1543_50_P_ W_870) shown in Fig. 6. Photographs of live ROV video monitors by JRP.

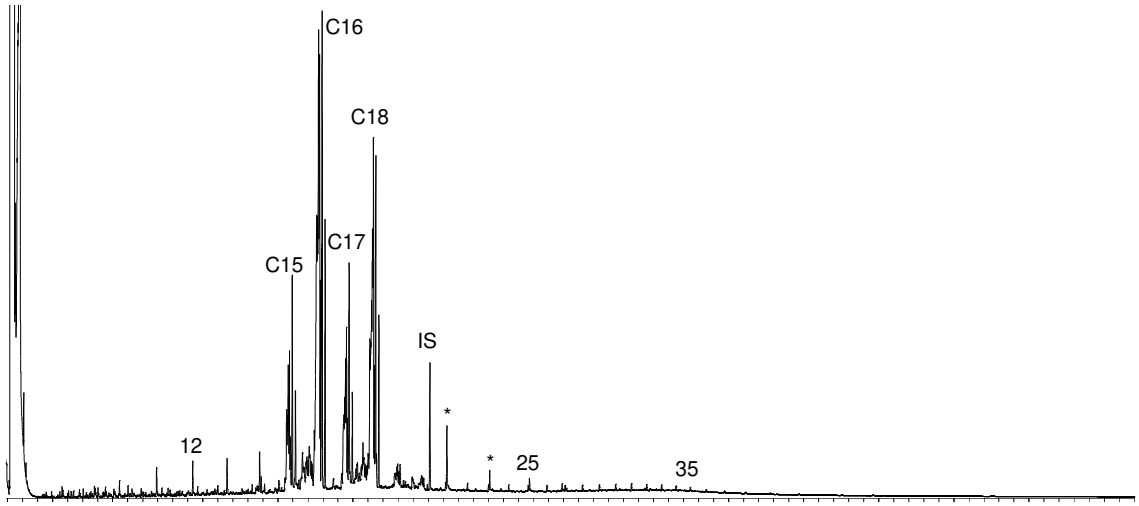

Fig. 6: GC-FID chromatogram of extractable material from a slurp gun filter sample containing SBM vacuumed from the seafloor (white particles from Fig. 5B). Sample is located 407 m southwest of the well in water depth of 1543 m; The %TPH as TPH_{SBM} in the sample is 93% (Table S-3) as 7% of the TPH is derived from crude oil that was also present in the vacuumed material. Sample ID: HSW2L2_FP0094_B0423_W_1543_ 50_P_W_870. #-*n*-alkane carbon number, C#-olefin cluster, IS-internal standard, * - C_{18} and C_{20} FAMEs.

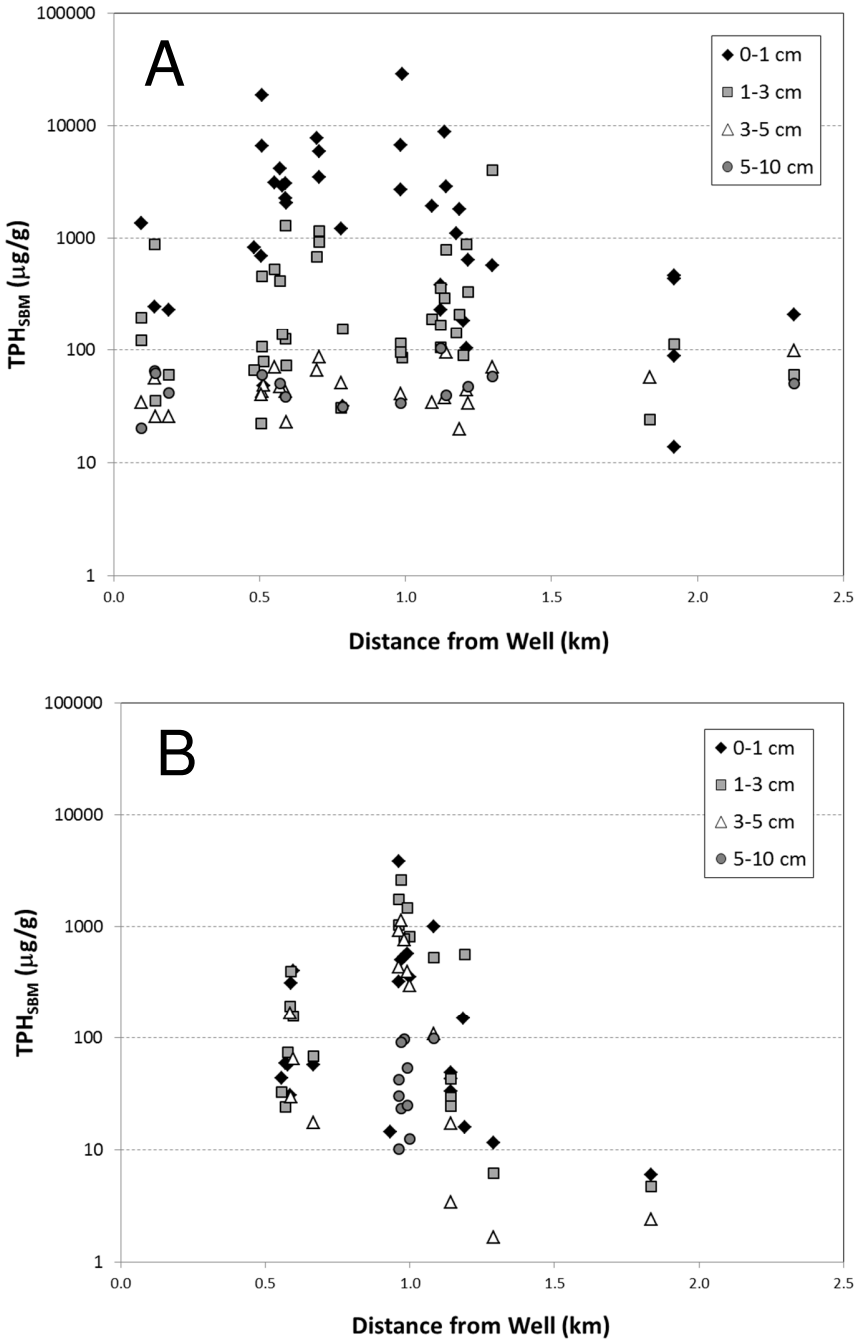

Figure 7: Total concentration of C_{14}-C_{20} olefins (TPH_{SBM}) in olefin-containing sediments collected at different sediment depth intervals and distances from the Macondo well in (A) 2010/2011 (n=118) and (B) 2014 (n=70). Data from Tables S-1 and S-2, respectively. Selected metrics by depth are given in Table 2.

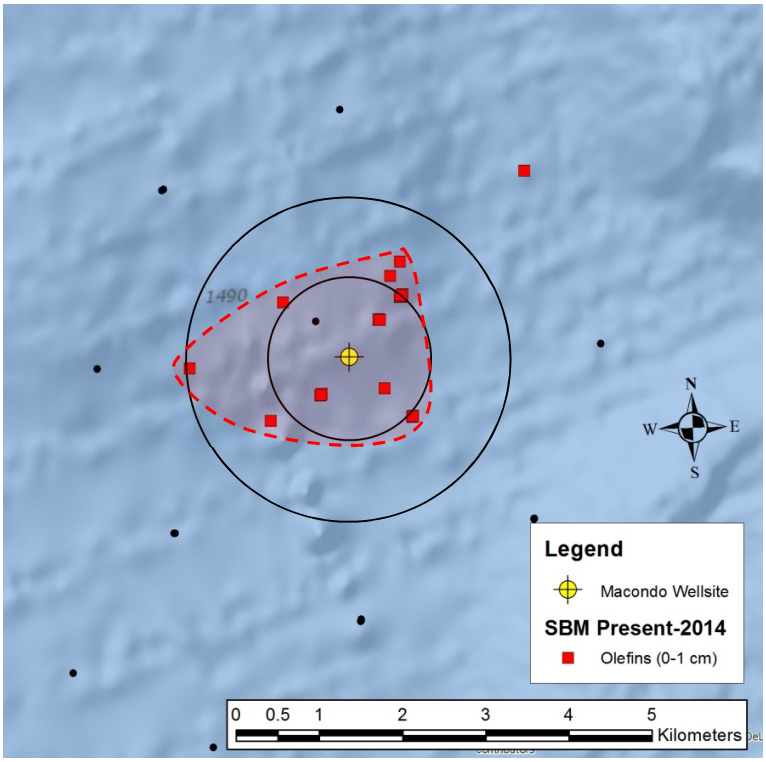

Figure 8: Map showing the cores collected in 2014 showing those containing SBM-derived olefins within an approximate 6.5 km^2 "footprint" of SBM-impacted sediments around the Macondo well. Black dots show all core locations with no olefins present. Circles depict 1 and 2 km radii from the well. See Table S-2 for an inventory of the 2014 cores and sediment intervals containing SBM-derived olefins.

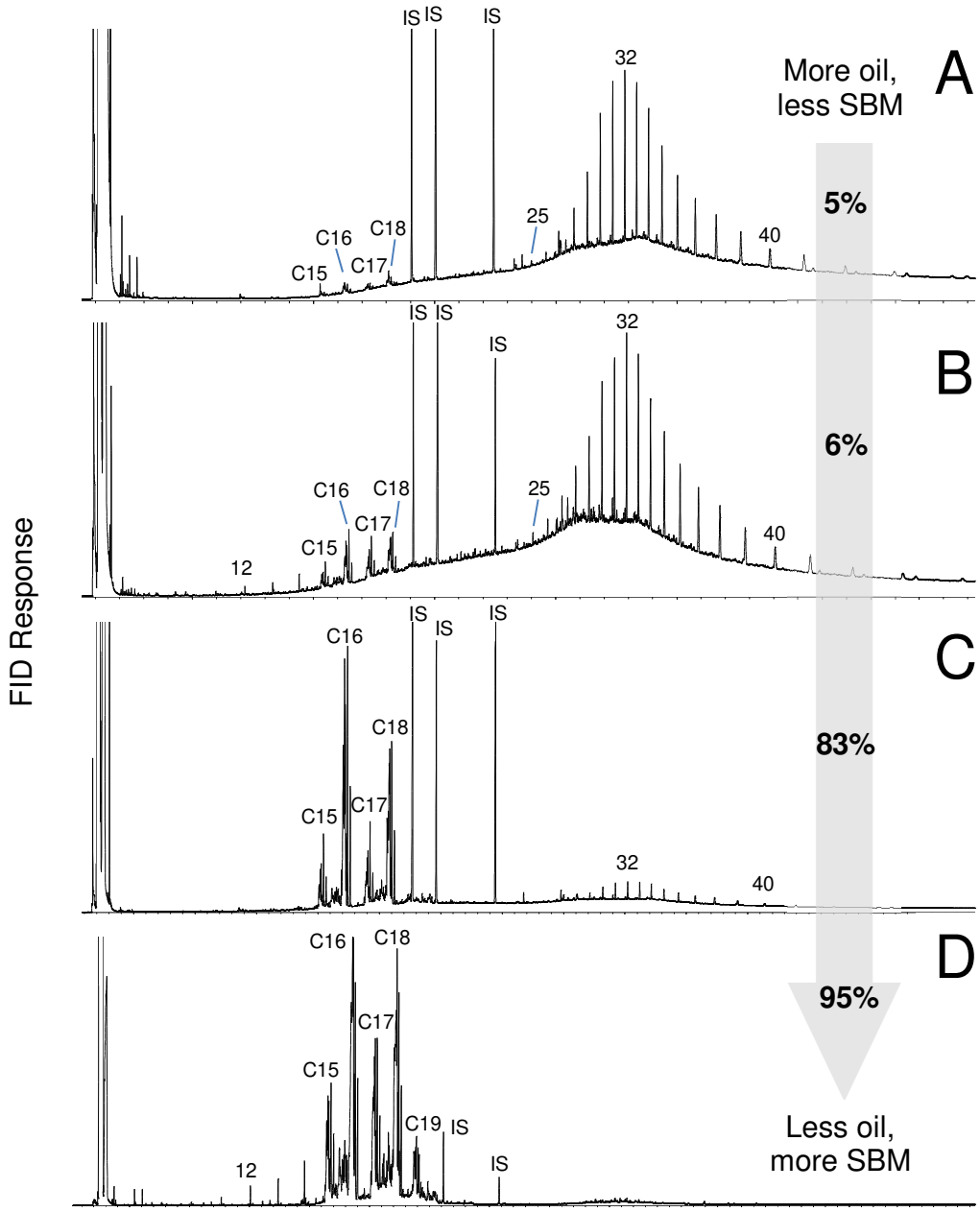

Figure 9: GC-FID chromatograms for sediments collected in 2014 showing persistence of SBM-derived olefins mixed with varying amounts of severely weathered crude oil. The %TPH as TPH_{SBM} in each is indicated along the arrow (per Table S-2). (A) RH1-65-E0604-S-D044S-HC-0931, (B) RH1-65-E0605-S-ALTNF001-HC-1043, (C) RH1-65-E0605-S-LBNL1-HC-1156, and (D) RH1-359-E0623-S-NF006MOD-HC-3732. #-*n*-alkane carbon number, C#-olefin cluster, IS-internal standard.

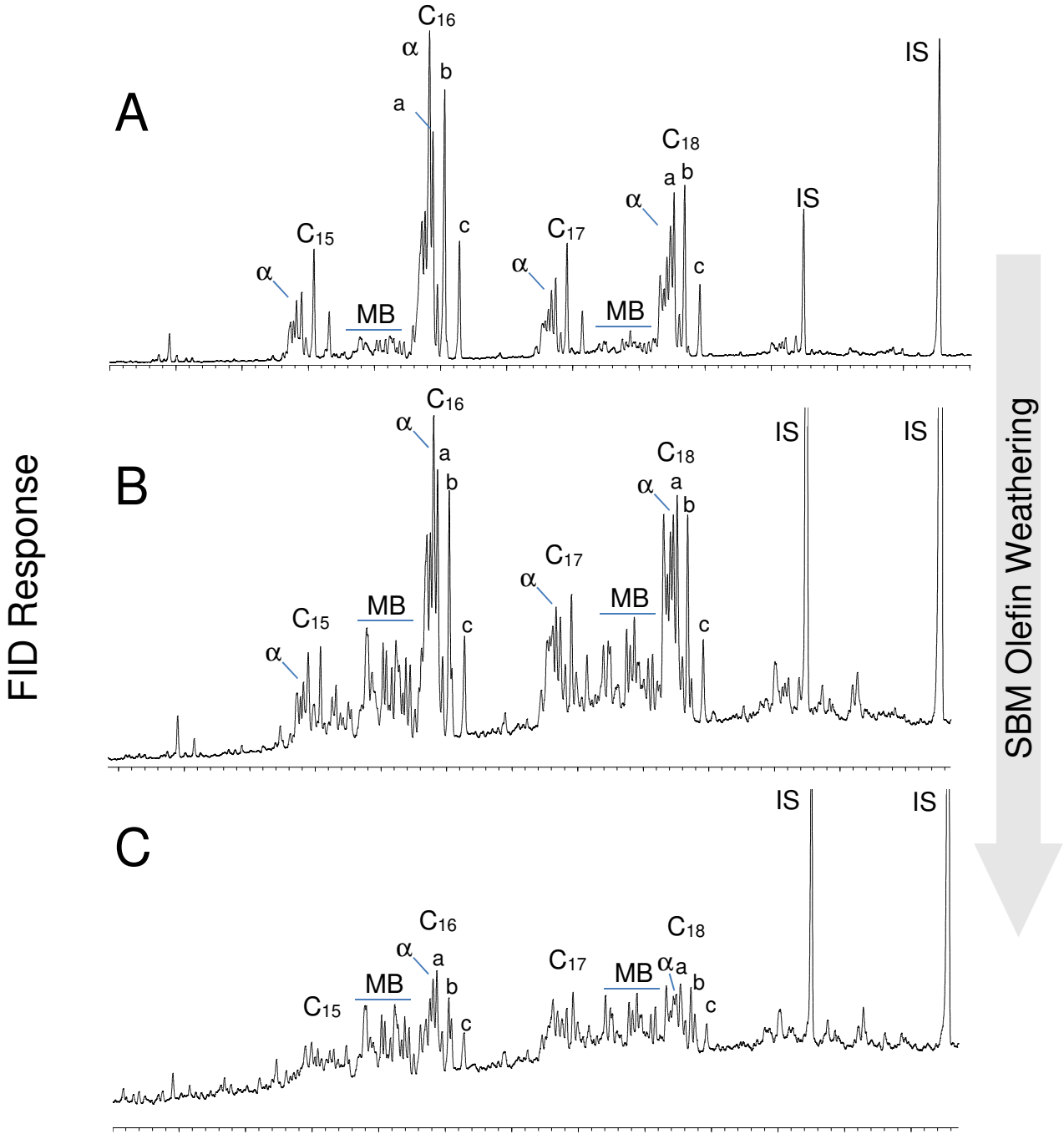

Figure 10: Partial GC-FID chromatogram of (A) minimally weathered SBM in sediment collected in 2014 (RH1-65-E0603-S-D040S-HC-0673), (B) intermediately weathered SBM in sediment collected in 2014 (RH1-65-E0603-S-D040S-HC-0702) and (C) highly weathered SBM in sediment collected in 2014 (RH1-65-E0604-S-D040S-HC-0730) showing the olefin clusters around C_{15}, C_{16}, C_{17}, and C_{18}. α - alpha olefins, MB – methyl-branched olefins, and a, b and c are unidentified internal olefin isomers. IS- internal standard. Note relative persistence of methyl-branched olefins in (C).

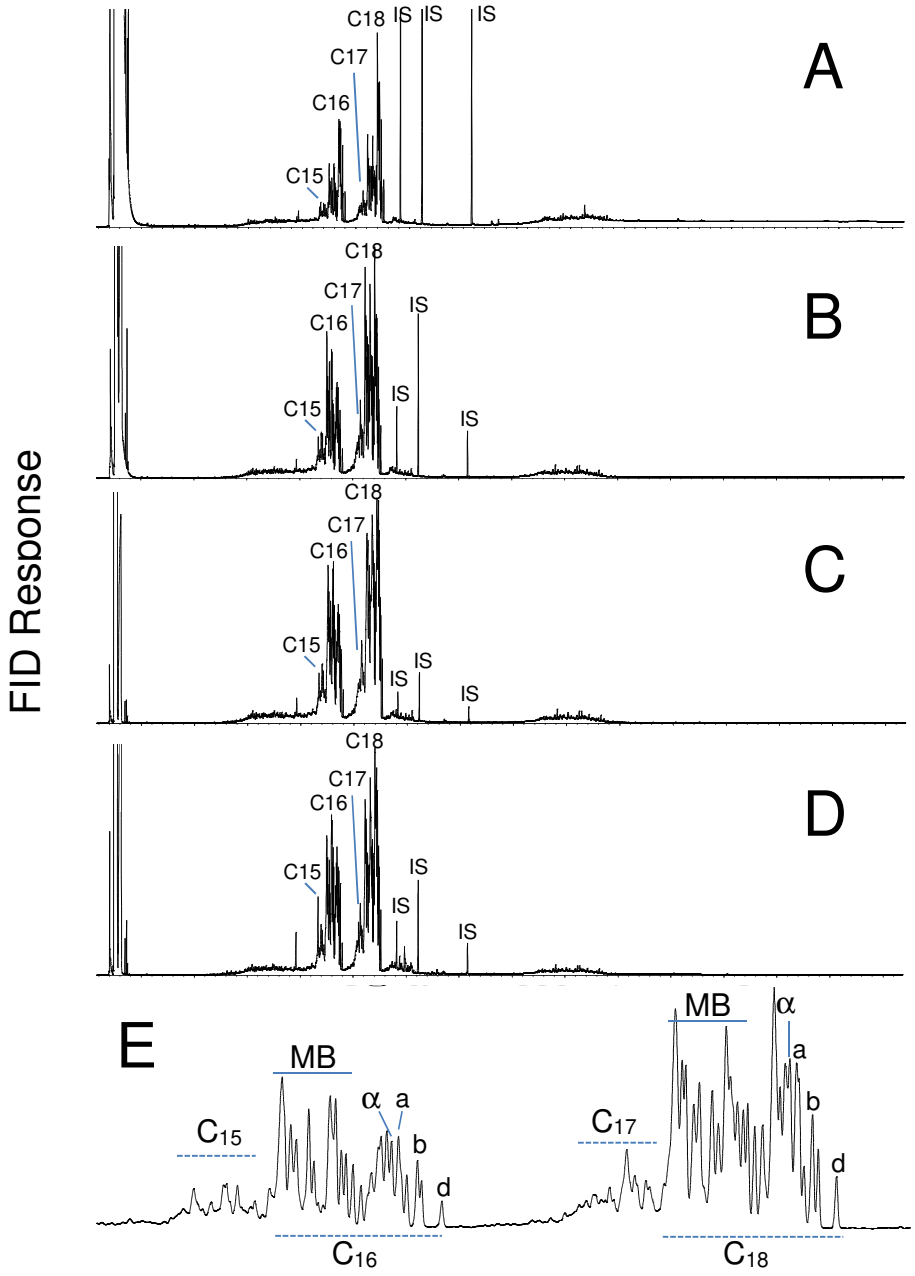

Figure 11: GC-FID chromatograms for sediments collected in 2011 from a core (SB9-65-B0608-S-VK916-HC-3454-3457) obtained near a former exploration well drilled in 2001 located 62 km northeast of the Macondo well. (A) 0-1 cm, (B) 1-3 cm, (C) 3-5 cm, and (D) 5-10 cm. (E) shows expanded view of olefins in (B). #-*n*-alkane carbon number, C#-olefin cluster, IS-internal standard. α - alpha olefins, MB – methyl-branched olefins, and a, b and c are unidentified internal olefin isomers. See text for description.

Supporting Information

Footprint, Weathering, and Persistence of Synthetic-Base Drilling Mud Olefins in Deep-Sea Sediments following the Deepwater Horizon Disaster

Scott A. Stout[a*] and James R. Payne[b]

[a] NewFields Environmental Forensics Practice, LLC, 300 Ledgewood Pl., Suite 305, Rockland, MA
[b] Payne Environmental Consultants, Inc. 1651 Linda Sue Ln., Encinitas, CA

5 Figures

3 Tables

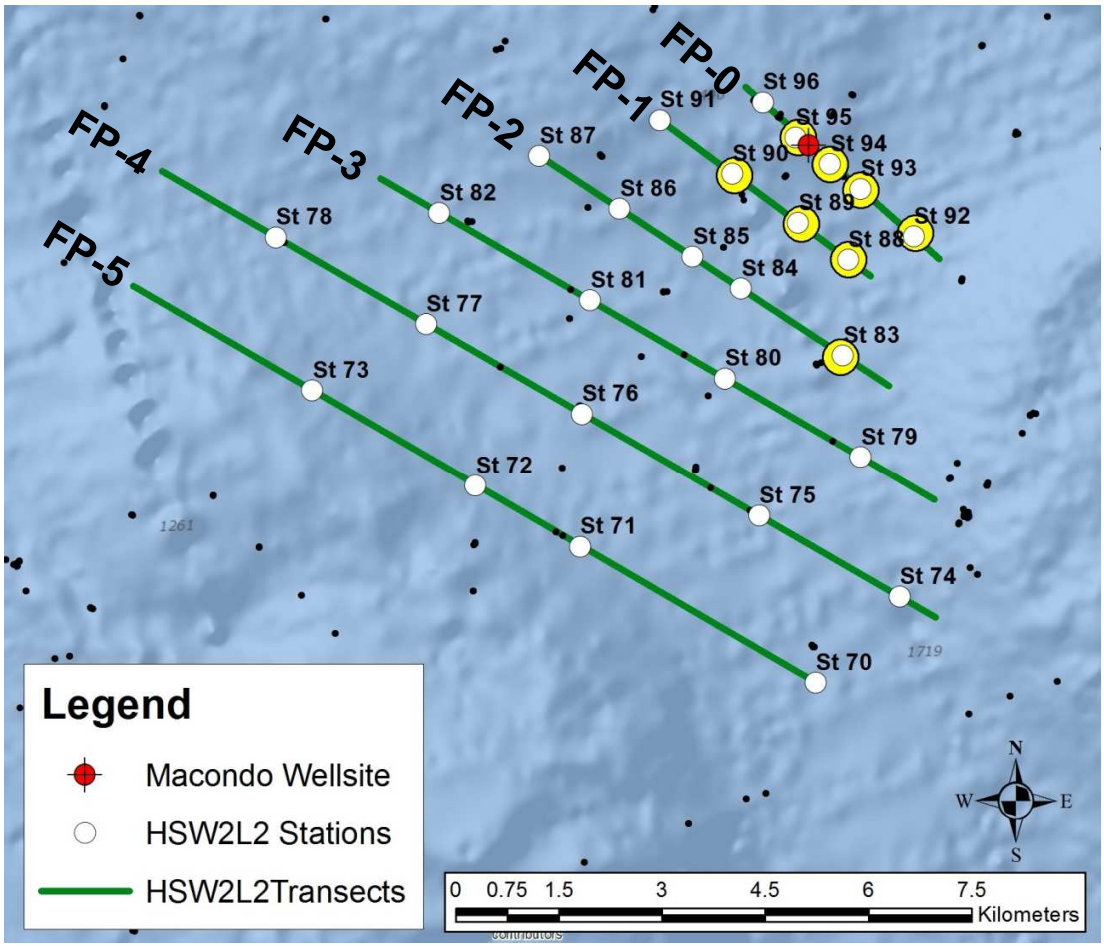

Fig. S-1. NW-SE trending transects (FP-0 to PF-6) and sampling stations investigated during the HOS Sweet Water 2 Leg 2 (HSW2L2) cruise in April 2011. The ROV video-camera system was used along each transect to continuously observe seafloor conditions and assist in the collection of sediment cores and slurp gun filter samples for chemical analysis. Sediment cores and slurp-gun filters were collected from each station, but SBM-enriched slurp gun filter samples were only targeted and obtained at eight stations along FP-0, FP-1, and FP-2 indicated by large circles (Table S-3). Black points show sediment core locations from other sampling cruises. Macondo oil residues in the other samples along the transects and other core locations are presented elsewhere (Stout and Payne, 2016; Stout et al., 2016). The ROV was "flown uphill" at 0.5 knots, 0.5-1 m above the seafloor from the SE to the NW as the sediment depths decreased by 80 to 210 m over the lengths of the respective transects.

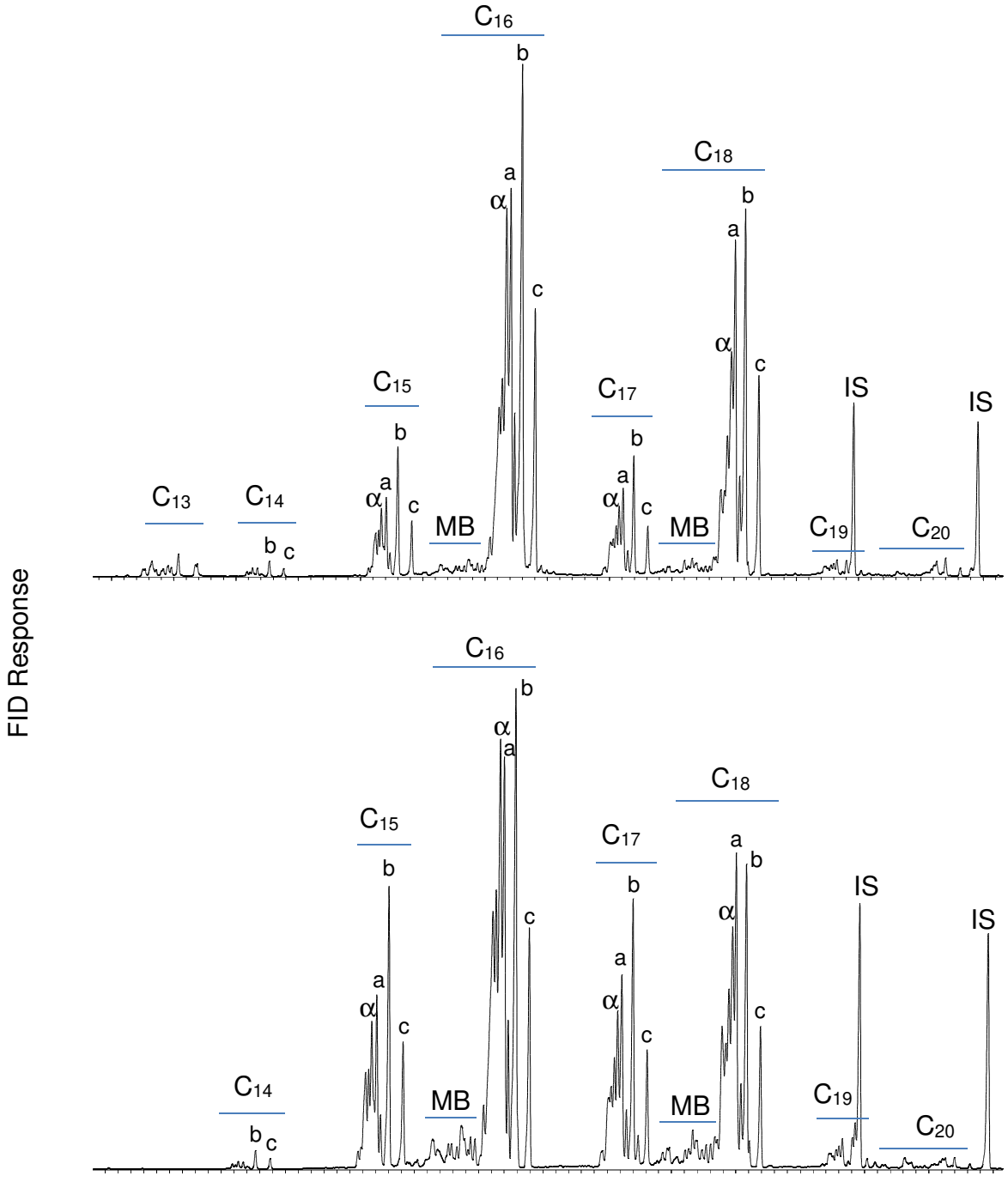

Fig. S-2: Partial GC-FID chromatograms of neat SBM from the (A) *Infant Jesus:* GU2909-A0602-OTARF2505B, (B) *Kylie Williams:* GU2909-A0602-OTARF2511. α - alpha olefins, MB – methyl-branched olefins, and a, b, and c are prominent internal olefin isomers (unidentified). IS-internal standard.

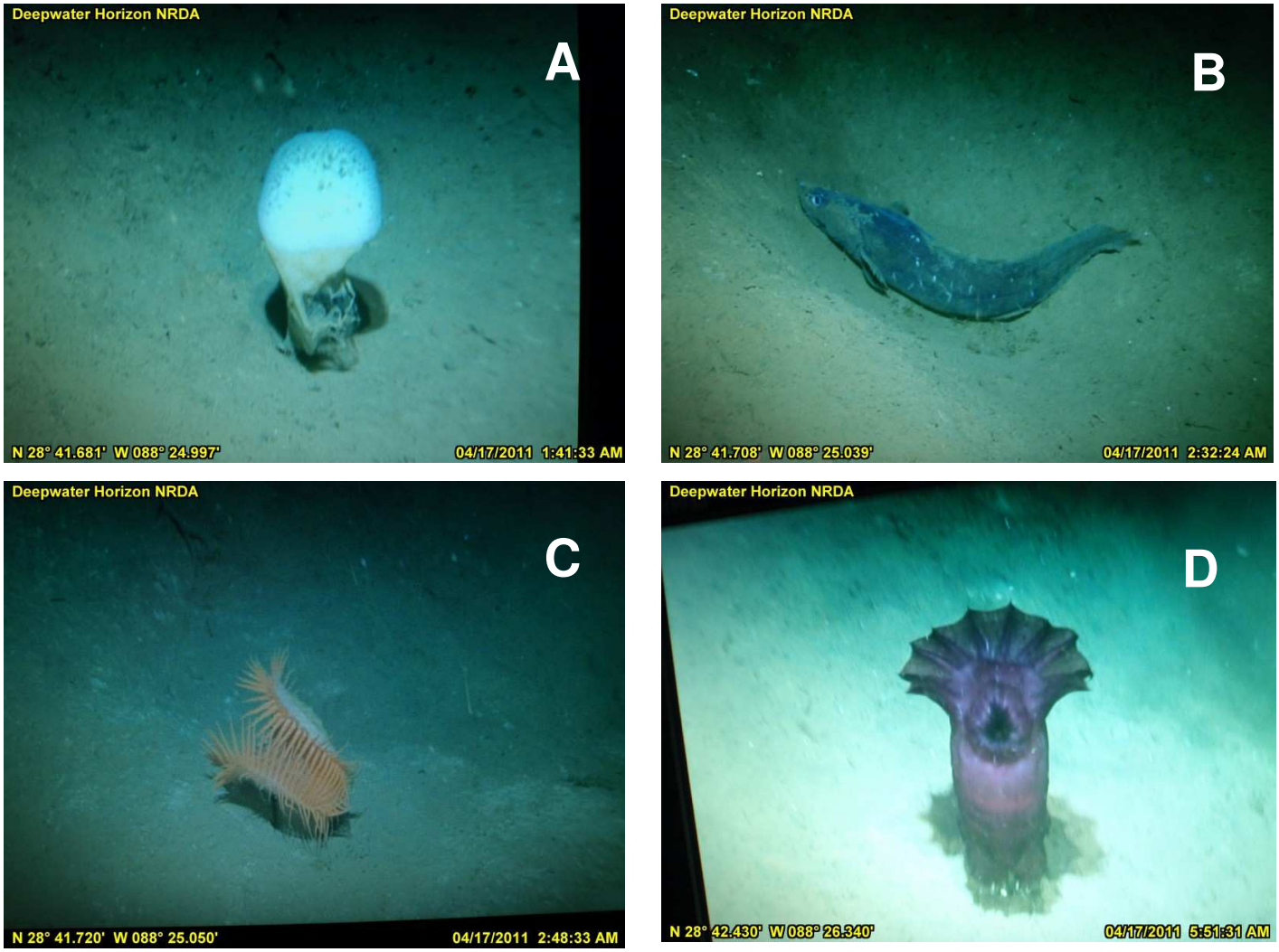

Fig. S-4: Photographs of bottom macrofauna observed along Transect FP-5 (A, B, C) near Station 72 (depth 1505 m) and (D) near Station 73 (depth 1417 m). No SBM layer was visually observed in this area and benthic macrofauna were more frequently observed than in transects FP-0 and FP-1 closer to the well where SBM deposition was extensive and nearly continuous (Figs. 3 and S-1). Photographs of live ROV video monitors by JRP.

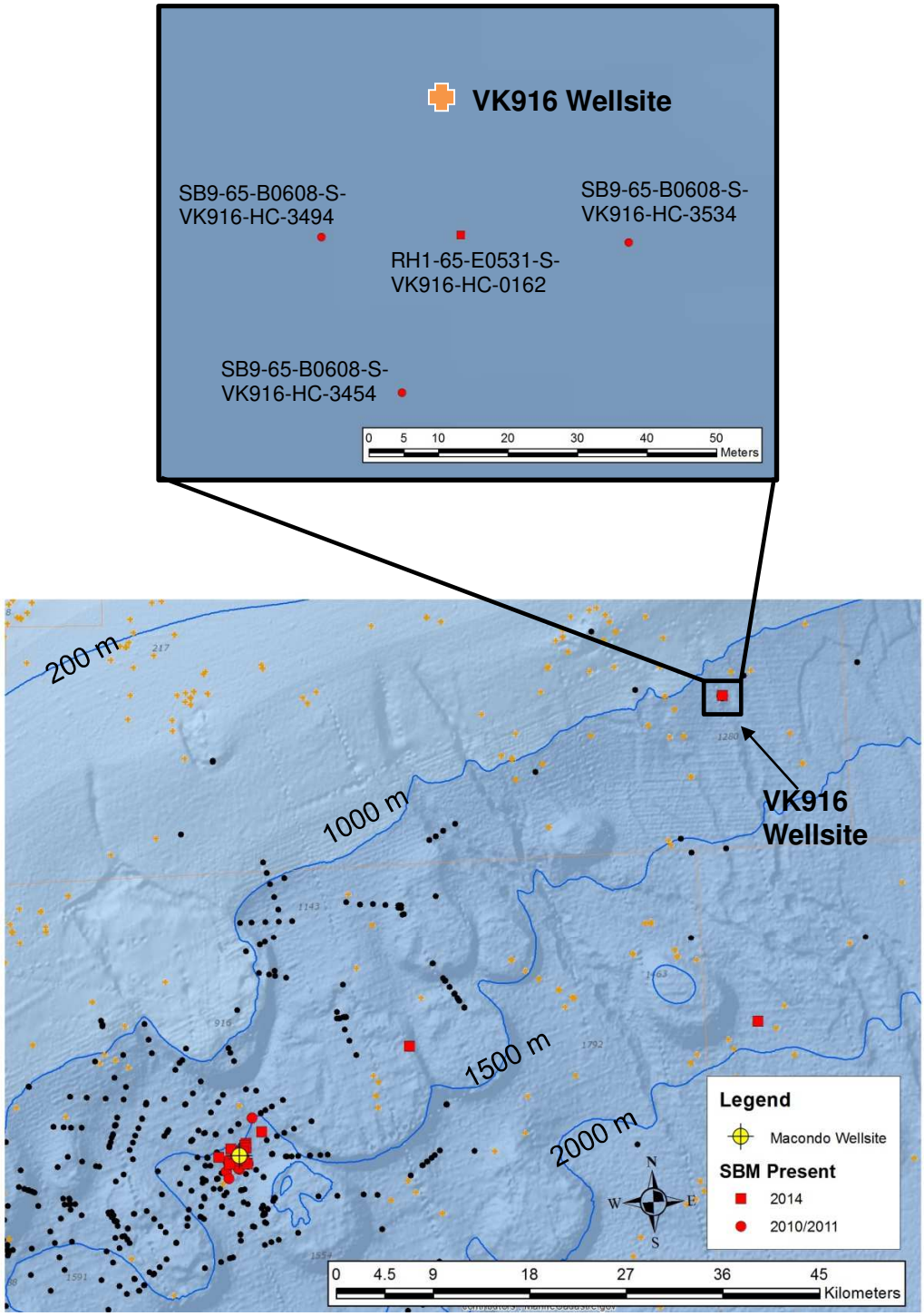

Fig. S-5: Map showing locations of all sediment cores (2010/2011 and 2014) containing SBM-derived olefins at the surface (0-1 cm) and known former drill site locations (https://www.data.boem.gov/homepg/data_center/well/well.asp). Inset shows four cores within 50 m of a 2001 well site in Viosca Knoll Block 916, 62 km from Macondo, containing olefins, which are 10 to 13 years old.

Table S-1: Inventory of samples collected from 2010/2011 containing SBM-derived olefins. Shaded rows at bottom of table are not attributed to DWH disaster.

Sample ID	latitude	longitude	Distance from Well (km)	Upper Depth (cm)	Lower Depth (cm)	TPH TOTAL (µg/g)	TPH SBM (µg/g)	%TPH as SBM
HSW2L2_FP0095_B0424_S_50_J2_875	28.73942	-88.36812	0.1	0	1	8870	1353	15
HSW2L2_FP0095_B0424_S_50_J3_875	28.73942	-88.36812	0.1	1	3	262	197	75
HSW2L2_FP0095_B0424_S_50_J4_875	28.73942	-88.36812	0.1	3	5	172	34	20
HSW2L2_FP0095_B0424_S_50_J5_875	28.73942	-88.36812	0.1	5	7	135	20	15
HSW2L2_FP0095_B0424_S_50_L2_877	28.73942	-88.36812	0.1	0	1	1558	1371	88
HSW2L2_FP0095_B0424_S_50_L3_877	28.73942	-88.36812	0.1	1	3	184	121	66
SB9-65-B0525-S-D038SW-HC-0026	28.73995	-88.36815	0.1	0	1	8149	244	3
SB9-65-B0525-S-D038SW-HC-0027	28.73995	-88.36815	0.1	1	3	1739	887	51
SB9-65-B0525-S-D038SW-HC-0028	28.73995	-88.36815	0.1	3	5	561	56	10
SB9-65-B0525-S-D038SW-HC-0029	28.73995	-88.36815	0.1	5	10	127	65	51
SB9-65-B0525-S-D038SW-HC-0065	28.73994	-88.36821	0.1	1	3	708	35	5
SB9-65-B0525-S-D038SW-HC-0066	28.73994	-88.36821	0.1	3	5	854	26	3
SB9-65-B0525-S-D038SW-HC-0067	28.73994	-88.36821	0.1	5	10	108	62	58
SB9-65-B0525-S-D038SW-HC-0104	28.74047	-88.36805	0.2	0	1	2303	230	10
SB9-65-B0525-S-D038SW-HC-0105	28.74047	-88.36805	0.2	1	3	1201	60	5
SB9-65-B0525-S-D038SW-HC-0106	28.74047	-88.36805	0.2	3	5	511	26	5
SB9-65-B0525-S-D038SW-HC-0107	28.74047	-88.36805	0.2	5	10	167	42	25
SB9-65-B0525-S-D042S-HC-0182	28.74211	-88.37066	0.5	0	1	2776	833	30
SB9-65-B0525-S-D042S-HC-0183	28.74211	-88.37066	0.5	1	3	1321	66	5
SB9-65-B0526-S-D042S-HC-0222	28.74220	-88.37094	0.5	0	1	2793	698	25
SB9-65-B0526-S-D042S-HC-0223	28.74220	-88.37094	0.5	1	3	447	22	5
SB9-65-B0526-S-D042S-HC-0224	28.74220	-88.37094	0.5	3	5	200	40	20
HSW2L2_FP0094_B0423_S_50_H4_868	28.73579	-88.36354	0.5	3	5	95	43	45
HSW2L2_FP0094_B0423_S_50_H5_868	28.73579	-88.36354	0.5	5	7	240	60	25
HSW2L2_FP0094_B0423_S_50_H2_868	28.73579	-88.36354	0.5	0	1	27371	18609	68
HSW2L2_FP0094_B0423_S_50_H3_868	28.73579	-88.36354	0.5	1	3	651	456	70
HSW2L2_FP0094_B0423_S_50_I2_869	28.73579	-88.36354	0.5	0	1	9690	6582	68
HSW2L2_FP0094_B0423_S_50_I3_869	28.73579	-88.36354	0.5	1	3	119	107	90
SB9-65-B0525-S-D042S-HC-0143	28.74260	-88.37053	0.5	0	1	1606	48	3
SB9-65-B0525-S-D042S-HC-0144	28.74260	-88.37053	0.5	1	3	188	79	42
SB9-65-B0525-S-D042S-HC-0145	28.74260	-88.37053	0.5	3	5	90	49	54
SB9-65-B0528-S-ALTNF001-HC-1207	28.73455	-88.37008	0.6	0	1	7779	3131	40
SB9-65-B0528-S-ALTNF001-HC-1208	28.73455	-88.37008	0.6	1	3	1511	529	35
SB9-65-B0528-S-ALTNF001-HC-1209	28.73455	-88.37008	0.6	3	5	140	70	50
SB9-65-B0529-S-ALTNF001-HC-1246	28.73443	-88.37021	0.6	0	1	9119	4199	46
SB9-65-B0529-S-ALTNF001-HC-1247	28.73443	-88.37021	0.6	1	3	1209	416	34
SB9-65-B0529-S-ALTNF001-HC-1248	28.73443	-88.37021	0.6	3	5	95	48	50
SB9-65-B0529-S-ALTNF001-HC-1249	28.73443	-88.37021	0.6	5	10	115	51	44
SB9-65-B0529-S-ALTNF001-HC-1285	28.73438	-88.37028	0.6	0	1	7516	2916	39
SB9-65-B0529-S-ALTNF001-HC-1286	28.73438	-88.37028	0.6	1	3	404	138	34
SB9-65-B0526-S-D040S-HC-0497	28.74228	-88.36273	0.6	0	1	5704	2282	40
SB9-65-B0526-S-D040S-HC-0498	28.74228	-88.36273	0.6	1	3	1373	1304	95
SB9-65-B0526-S-D040S-HC-0499	28.74228	-88.36273	0.6	3	5	77	43	56

Sample ID	latitude	longitude	Distance from Well (km)	Upper Depth (cm)	Lower Depth (cm)	TPH TOTAL (µg/g)	TPH SBM (µg/g)	%TPH as SBM
SB9-65-B0526-S-D040S-HC-0500	28.74228	-88.36273	0.6	5	10	85	38	45
SB9-65-B0527-S-D040S-HC-0536	28.74226	-88.36268	0.6	0	1	14013	3099	22
SB9-65-B0527-S-D040S-HC-0537	28.74226	-88.36268	0.6	1	3	417	125	30
SB9-65-B0527-S-D040S-HC-0576	28.74232	-88.36270	0.6	0	1	6826	2048	30
SB9-65-B0527-S-D040S-HC-0577	28.74232	-88.36270	0.6	1	3	363	73	20
SB9-65-B0527-S-D040S-HC-0578	28.74232	-88.36270	0.6	3	5	115	23	20
SB9-65-B0528-S-D034S-HC-1047	28.73438	-88.36243	0.7	0	1	42129	7791	18
SB9-65-B0528-S-D034S-HC-1048	28.73438	-88.36243	0.7	1	3	1647	679	41
SB9-65-B0528-S-D034S-HC-1049	28.73438	-88.36243	0.7	3	5	127	66	52
SB9-65-B0528-S-D034S-HC-0969	28.73432	-88.36239	0.7	0	1	22058	1629	7
SB9-65-B0528-S-D034S-HC-0970	28.73432	-88.36239	0.7	1	3	1694	1152	68
SB9-65-B0528-S-D034S-HC-1008	28.73433	-88.36237	0.7	0	1	20790	5950	29
SB9-65-B0528-S-D034S-HC-1009	28.73433	-88.36237	0.7	1	3	2372	925	39
SB9-65-B0528-S-D034S-HC-1010	28.73433	-88.36237	0.7	3	5	248	87	35
HSW2L2_FP0093A_B0423_S_50_G2_863	28.73408	-88.36156	0.8	0	1	3945	1211	31
HSW2L2_FP0093A_B0423_S_50_G3_863	28.73408	-88.36156	0.8	1	3	308	31	10
HSW2L2_FP0093A_B0423_S_50_G4_863	28.73408	-88.36156	0.8	3	5	85	51	60
HSW2L2_FP0096_B0424_S_50_N2_885	28.74384	-88.37310	0.8	0	1	630	31	5
HSW2L2_FP0096_B0424_S_50_N5_885	28.74384	-88.37310	0.8	5	7	155	31	20
HSW2L2_FP0096_B0424_S_50_Q3_887	28.74384	-88.37310	0.8	1	3	256	153	60
SB9-65-B0526-S-NF006MOD-HC-0458	28.74482	-88.35988	1.0	0	1	2826	2685	95
SB9-65-B0526-S-NF006MOD-HC-0459	28.74482	-88.35988	1.0	1	3	238	95	40
SB9-65-B0526-S-NF006MOD-HC-0460	28.74482	-88.35988	1.0	3	5	103	41	40
SB9-65-B0526-S-NF006MOD-HC-0461	28.74482	-88.35988	1.0	5	10	80	34	42
SB9-65-B0526-S-NF006MOD-HC-0419	28.74479	-88.35983	1.0	0	1	8271	6785	82
SB9-65-B0526-S-NF006MOD-HC-0420	28.74479	-88.35983	1.0	1	3	377	113	30
SB9-65-B0526-S-NF006MOD-HC-0379	28.74474	-88.35973	1.0	0	1	29848	28654	96
SB9-65-B0526-S-NF006MOD-HC-0380	28.74474	-88.35973	1.0	1	3	215	86	40
HSW2L2_FP0093_B0423_S_50_E2_859	28.73225	-88.35915	1.1	0	1	13755	1936	14
HSW2L2_FP0093_B0423_S_50_E3_859	28.73225	-88.35915	1.1	1	3	921	189	20
HSW2L2_FP0093_B0423_S_50_E4_859	28.73225	-88.35915	1.1	3	5	115	35	30
HSW2L2_FP1090_B0423_S_50_H2_824	28.73484	-88.37786	1.1	0	1	1366	382	28
HSW2L2_FP1090_B0423_S_50_H3_824	28.73484	-88.37786	1.1	1	3	322	167	52
HSW2L2_FP1090_B0423_S_50_I3_825	28.73484	-88.37786	1.1	1	3	428	360	84
HSW2L2_FP1090_B0423_S_50_K2_826	28.73484	-88.37786	1.1	0	1	562	231	41
HSW2L2_FP1090_B0423_S_50_K3_826	28.73484	-88.37786	1.1	1	3	130	105	81
HSW2L2_FP1090_B0423_S_50_H5_824	28.73484	-88.37786	1.1	5	7	170	104	61
SB9-65-B0528-S-D031S-HC-1087	28.73164	-88.35920	1.1	0	1	26488	8895	34
SB9-65-B0528-S-D031S-HC-1088	28.73164	-88.35920	1.1	1	3	2920	292	10
SB9-65-B0528-S-D031S-HC-1089	28.73164	-88.35920	1.1	3	5	75	38	50
SB9-65-B0528-S-D031S-HC-1167	28.73211	-88.35862	1.1	0	1	12288	2898	24
SB9-65-B0528-S-D031S-HC-1168	28.73211	-88.35862	1.1	1	3	3171	790	25
SB9-65-B0528-S-D031S-HC-1169	28.73211	-88.35862	1.1	3	5	241	96	40
SB9-65-B0528-S-D031S-HC-1170	28.73211	-88.35862	1.1	5	10	62	40	64
SB9-65-B0602-S-LBNL1-HC-1404	28.73228	-88.37673	1.2	0	1	2160	1102	51
SB9-65-B0602-S-LBNL1-HC-1405	28.73228	-88.37673	1.2	1	3	296	142	48
SB9-65-B0528-S-D031S-HC-1127	28.73128	-88.35887	1.2	0	1	11433	1815	16

Sample ID	latitude	longitude	Distance from Well (km)	Upper Depth (cm)	Lower Depth (cm)	TPH TOTAL (µg/g)	TPH SBM (µg/g)	%TPH as SBM
SB9-65-B0528-S-D031S-HC-1128	28.73128	-88.35887	1.2	1	3	3352	208	6
SB9-65-B0528-S-D031S-HC-1129	28.73128	-88.35887	1.2	3	5	200	20	10
HSW2L2_FP1089_B0423_S_50_G2_817	28.72815	-88.36819	1.2	0	1	352	183	52
HSW2L2_FP1089_B0423_S_50_G3_817	28.72815	-88.36819	1.2	1	3	165	89	54
SB9-65-B0529-S-LBNL1-HC-1365	28.73158	-88.37651	1.2	1	3	1999	887	44
SB9-65-B0529-S-LBNL1-HC-1366	28.73158	-88.37651	1.2	3	5	99	44	45
SB9-65-B0529-S-LBNL1-HC-1368	28.73158	-88.37651	1.2	0	1	200	104	52
SB9-65-B0529-S-LBNL1-HC-1325	28.73155	-88.37657	1.2	0	1	1604	642	40
SB9-65-B0529-S-LBNL1-HC-1326	28.73155	-88.37657	1.2	1	3	550	335	61
SB9-65-B0529-S-LBNL1-HC-1327	28.73155	-88.37657	1.2	3	5	43	34	78
SB9-65-B0529-S-LBNL1-HC-1328	28.73155	-88.37657	1.2	5	10	94	47	50
HSW2L2_FP1088A_B0423_S_50_D2_810	28.72724	-88.36695	1.3	0	1	16200	575	4
HSW2L2_FP1088A_B0423_S_50_D3_810	28.72724	-88.36695	1.3	1	3	4280	4066	95
HSW2L2_FP1088A_B0423_S_50_D4_810	28.72724	-88.36695	1.3	3	5	226	70	31
HSW2L2_FP1088A_B0423_S_50_D5_810	28.72724	-88.36695	1.3	5	7	165	58	35
HSW2L2_FP1088_B0423_S_50_A3_806	28.72323	-88.36140	1.8	1	3	80	24	30
HSW2L2_FP1088_B0423_S_50_A4_806	28.72323	-88.36140	1.8	3	5	130	57	44
HD5_HD5004_A1214_S_BR2_01	28.72550	-88.37980	1.9	0	1	1038	89	9
HD5_HD5004_A1214_S_GR2_04	28.72550	-88.37980	1.9	0	1	459	436	95
HD5_HD5004_A1214_S_GR4_04	28.72550	-88.37980	1.9	2	4	200	112	56
HD5_HD5004_A1214_S_PU2_03	28.72550	-88.37980	1.9	0	1	502	462	92
HD5_HD5004_A1214_S_YW2_05	28.72550	-88.37980	1.9	0	1	440	14	3
HSW2L2_FP2084_B0422_S_50_D3_771	28.71976	-88.37710	2.3	1	3	98	60	61
HSW2L2_FP2084_B0422_S_50_D4_771	28.71976	-88.37710	2.3	3	5	223	98	44
HSW2L2_FP2084_B0422_S_50_D5_771	28.71976	-88.37710	2.3	5	7	179	50	28
HSW2L2_FP2084_B0422_S_50_F2_773	28.71976	-88.37710	2.3	0	1	439	211	48
HSW6_FP10188_B0827_S_1485_50_H2_0072	28.76980	-88.35320	3.7	0	1	61886	5343	9
HSW6_FP10188_B0827_S_1485_50_H3_0072	28.76980	-88.35320	3.7	1	3	2839	1561	55
HSW2L2_FP3080A_B0419_S_50_I3_692	28.71161	-88.38621	3.5	1	3	115	44	38
HSW2L2_FP3080A_B0419_S_50_I4_692	28.71161	-88.38621	3.5	3	5	155	26	17
HSW2L2_FP3080A_B0419_S_50_I5_692	28.71161	-88.38621	3.5	5	7	650	487	75
HD5_HD5005_A1215_S_PU5_04	28.71160	-88.39260	3.9	4	6	68	65	95
HD5_HD5005_A1215_S_PU6_04	28.71160	-88.39260	3.9	6	10	65	55	84
HD5_HD5006_A1215_S_BR7_02	28.71698	-88.40302	4.2	4	6	53	22	41
HD5_HD5003_A1211_S_BL3_05	28.69740	-88.40500	5.9	2	4	64	61	95
HD5_HD5003_A1211_S_BL4_05	28.69740	-88.40500	5.9	4	6	70	67	95
HD5_HD5003_A1211_S_GR6_04	28.69740	-88.40500	5.9	6	10	80	76	95
SB9-65-B0606-S-FF005-HC-2943	28.80296	-88.56454	20	3	5	54	22	40
SB9-65-B0606-S-FF005-HC-2944	28.80296	-88.56454	20	5	10	55	32	58
SB9-65-B0606-S-FF005-HC-2904	28.80312	-88.56505	21	3	5	95	41	43
SB9-65-B0606-S-FF005-HC-2905	28.80312	-88.56505	21	5	10	89	48	54
SB9-65-B0608-S-VK916-HC-3454	29.10662	-87.88882	62	0	1	438	228	52
SB9-65-B0608-S-VK916-HC-3455	29.10662	-87.88882	62	1	3	1340	1219	91
SB9-65-B0608-S-VK916-HC-3456	29.10662	-87.88882	62	3	5	2253	1059	47
SB9-65-B0608-S-VK916-HC-3457	29.10662	-87.88882	62	5	10	1142	434	38
SB9-65-B0608-S-VK916-HC-3494	29.10682	-87.88892	62	0	1	108	52	48
SB9-65-B0608-S-VK916-HC-3495	29.10682	-87.88892	62	1	3	186	84	45

Sample ID	latitude	longitude	Distance from Well (km)	Upper Depth (cm)	Lower Depth (cm)	TPH TOTAL (µg/g)	TPH SBM (µg/g)	%TPH as SBM
SB9-65-B0608-S-VK916-HC-3496	29.10682	-87.88892	62	3	5	72	56	78
SB9-65-B0608-S-VK916-HC-3497	29.10682	-87.88892	62	5	10	215	73	34
SB9-65-B0608-S-VK916-HC-3534	29.10680	-87.88847	62	0	1	361	325	90
SB9-65-B0608-S-VK916-HC-3535	29.10680	-87.88847	62	1	3	305	152	50
SB9-65-B0608-S-VK916-HC-3536	29.10680	-87.88847	62	3	5	172	95	55
SB9-65-B0608-S-VK916-HC-3537	29.10680	-87.88847	62	5	10	240	106	44

Table S-2: Inventory of samples collected from 2014 containing SBM-derived olefins. Shaded rows at bottom of table are not attributed to DWH disaster.

Sample ID	latitude	longitude	Distance from Well (km)	Upper Depth (cm)	Lower Depth (cm)	TPH TOTAL (µg/g)	TPH SBM (µg/g)	%TPH as SBM
RH1-65-E0605-S-ALTNF001-HC-1013	28.73449	-88.37006	0.6	0	1	730	44	6
RH1-65-E0605-S-ALTNF001-HC-1014	28.73449	-88.37006	0.6	1	3	274	33	12
RH1-65-E0605-S-ALTNF001-HC-1070	28.73441	-88.37018	0.6	0	1	984	59	6
RH1-65-E0605-S-ALTNF001-HC-1071	28.73441	-88.37018	0.6	1	3	404	24	6
RH1-65-E0605-S-ALTNF001-HC-1043	28.73434	-88.37022	0.6	0	1	959	58	6
RH1-65-E0605-S-ALTNF001-HC-1044	28.73434	-88.37022	0.6	1	3	491	74	15
RH1-65-E0603-S-D040S-HC-0671	28.74228	-88.36276	0.6	0	1	647	31	5
RH1-65-E0603-S-D040S-HC-0672	28.74228	-88.36276	0.6	1	3	1596	193	12
RH1-65-E0603-S-D040S-HC-0673	28.74228	-88.36276	0.6	3	5	361	168	47
RH1-65-E0603-S-D040S-HC-0702	28.74229	-88.36274	0.6	0	1	1168	310	27
RH1-65-E0603-S-D040S-HC-0703	28.74229	-88.36274	0.6	1	3	1318	397	30
RH1-65-E0603-S-D040S-HC-0704	28.74229	-88.36274	0.6	3	5	100	30	30
RH1-65-E0604-S-D040S-HC-0729	28.74223	-88.36257	0.6	0	1	1012	406	40
RH1-65-E0604-S-D040S-HC-0730	28.74223	-88.36257	0.6	1	3	1043	156	15
RH1-65-E0604-S-D040S-HC-0731	28.74223	-88.36257	0.6	3	5	129	65	50
RH1-65-E0603-S-D034S-HC-0643	28.73486	-88.36231	0.7	0	1	1920	58	3
RH1-65-E0603-S-D034S-HC-0644	28.73486	-88.36231	0.7	1	3	2288	69	3
RH1-65-E0603-S-D034S-HC-0645	28.73486	-88.36231	0.7	3	5	158	17	11
RH1-65-E0604-S-D044S-HC-0931	28.74456	-88.3744	0.9	0	1	288	14	5
RH1-359-E0623-S-NF006MOD-HC-3732	28.74465	-88.36	1.0	0	1	4027	3826	95
RH1-359-E0623-S-NF006MOD-HC-3733	28.74465	-88.36	1.0	1	3	1968	1771	90
RH1-359-E0623-S-NF006MOD-HC-3734	28.74465	-88.36	1.0	3	5	1237	928	75
RH1-359-E0623-S-NF006MOD-HC-3735	28.74465	-88.36	1.0	5	10	78	42	54
RH1-359-E0623-S-NF006MOD-HC-3736	28.74465	-88.36	1.0	10	15	200	30	15
RH1-359-E0623-S-NF006MOD-HC-3789	28.7447	-88.36002	1.0	0	1	351	323	92
RH1-359-E0623-S-NF006MOD-HC-3790	28.7447	-88.36002	1.0	1	3	1102	1036	94
RH1-359-E0623-S-NF006MOD-HC-3791	28.7447	-88.36002	1.0	3	5	517	439	85
RH1-359-E0623-S-NF006MOD-HC-3792	28.7447	-88.36002	1.0	5	10	46	10	22
RH1-359-E0623-S-NF006MOD-HC-3755	28.74466	-88.35988	1.0	0	1	569	507	89
RH1-359-E0623-S-NF006MOD-HC-3756	28.74466	-88.35988	1.0	1	3	2934	2641	90
RH1-359-E0623-S-NF006MOD-HC-3757	28.74466	-88.35988	1.0	3	5	1422	1138	80
RH1-359-E0623-S-NF006MOD-HC-3758	28.74466	-88.35988	1.0	5	10	59	24	40
RH1-359-E0623-S-NF006MOD-HC-3759	28.74466	-88.35988	1.0	10	15	175	91	52
RH1-359-E0623-S-NF006MOD-HC-3860	28.74483	-88.35993	1.0	0	1	564	536	95
RH1-359-E0623-S-NF006MOD-HC-3861	28.74483	-88.35993	1.0	1	3	796	780	98
RH1-359-E0623-S-NF006MOD-HC-3862	28.74483	-88.35993	1.0	3	5	855	770	90
RH1-359-E0623-S-NF006MOD-HC-3863	28.74483	-88.35993	1.0	5	10	122	97	80
RH1-359-E0623-S-NF006MOD-HC-3826	28.74481	-88.35975	1.0	0	1	592	574	97
RH1-359-E0623-S-NF006MOD-HC-3827	28.74481	-88.35975	1.0	1	3	1501	1471	98
RH1-359-E0623-S-NF006MOD-HC-3828	28.74481	-88.35975	1.0	3	5	672	397	59
RH1-359-E0623-S-NF006MOD-HC-3829	28.74481	-88.35975	1.0	5	10	87	54	62
RH1-359-E0623-S-NF006MOD-HC-3830	28.74481	-88.35975	1.0	10	15	61	25	41
RH1-359-E0623-S-NF006MOD-HC-3705	28.74489	-88.35971	1.0	0	1	497	358	72
RH1-359-E0623-S-NF006MOD-HC-3706	28.74489	-88.35971	1.0	1	3	1451	817	56

Sample ID	latitude	longitude	Distance from Well (km)	Upper Depth (cm)	Lower Depth (cm)	TPH TOTAL (µg/g)	TPH SBM (µg/g)	%TPH as SBM
RH1-359-E0623-S-NF006MOD-HC-3707	28.74489	-88.35971	1.0	3	5	456	296	65
RH1-359-E0623-S-NF006MOD-HC-3708	28.74489	-88.35971	1.0	5	10	50	12	25
RH1-359-E0623-S-MC253-NESW5-HC-3879	28.74695	-88.36113	1.1	0	1	1058	1005	95
RH1-359-E0623-S-MC253-NESW5-HC-3880	28.74695	-88.36113	1.1	1	3	573	533	93
RH1-359-E0623-S-MC253-NESW5-HC-3881	28.74695	-88.36113	1.1	3	5	167	109	65
RH1-359-E0623-S-MC253-NESW5-HC-3882	28.74695	-88.36113	1.1	5	10	185	98	53
RH1-65-E0603-S-D031S-HC-0589	28.73173	-88.35899	1.1	0	1	979	49	5
RH1-65-E0603-S-D031S-HC-0590	28.73173	-88.35899	1.1	1	3	816	24	3
RH1-65-E0603-S-D031S-HC-0591	28.73173	-88.35899	1.1	3	5	86	3	4
RH1-65-E0603-S-D031S-HC-0616	28.73172	-88.359	1.1	0	1	721	43	6
RH1-65-E0603-S-D031S-HC-0617	28.73172	-88.359	1.1	1	3	718	43	6
RH1-65-E0603-S-D031S-HC-0618	28.73172	-88.359	1.1	3	5	343	17	5
RH1-65-E0603-S-D031S-HC-0559	28.73164	-88.35908	1.1	0	1	1112	33	3
RH1-65-E0603-S-D031S-HC-0560	28.73164	-88.35908	1.1	1	3	974	29	3
RH1-65-E0605-S-LBNL1-HC-1128	28.73183	-88.37646	1.2	0	1	359	151	42
RH1-65-E0605-S-LBNL1-HC-1155	28.73179	-88.37646	1.2	0	1	319	16	5
RH1-65-E0605-S-LBNL1-HC-1156	28.73179	-88.37646	1.2	1	3	686	569	83
RH1-359-E0623-S-MC253-NESW1-HC-3896	28.74845	-88.35988	1.3	0	1	166	12	7
RH1-359-E0623-S-MC253-NESW1-HC-3897	28.74845	-88.35988	1.3	1	3	124	6	5
RH1-359-E0623-S-MC253-NESW1-HC-3898	28.74845	-88.35988	1.3	3	5	56	2	3
RH1-359-E0624-S-21-HC-3967	28.73781	-88.38613	1.8	0	1	201	6	3
RH1-359-E0624-S-21-HC-3968	28.73781	-88.38613	1.8	1	3	157	5	3
RH1-359-E0624-S-21-HC-3969	28.73781	-88.38613	1.8	3	5	48	2	5
RH1-359-E0621-S-NF012-HC-3659	28.75782	-88.34417	3.1	0	1	256	133	52
RH1-65-E0602-S-MF002-HC-0362	28.82431	-88.20045	19	0	1	200	20	10
RH1-65-E0601-S-D009S-HC-0246	28.83319	-87.86832	50	0	1	200	124	62
RH1-65-E0531-S-VK916-HC-0162	29.10682	-87.88872	62	0	1	180	45	25
RH1-65-E0531-S-VK916-HC-0163	29.10682	-87.88872	62	1	3	44	7	17
RH1-65-E0531-S-VK916-HC-0164	29.10682	-87.88872	62	3	5	200	10	5
RH1-65-E0531-S-VK916-HC-0165	29.10682	-87.88872	62	5	10	180	9	5

Table S-3: Inventory of eight slurp gun filter samples collected in April 2011 that attempted to surgically collect white, star-like material rich in SBM-derived olefins.

Slurp Gun Filter Sample ID	latitude	longitude	Water Depth (m)	TPH (µg/filter)	TPH SBM (µg/filter)	%TPH as SBM
HSW2L2_FP2083_B0422_W_1606_50_P_U_766	28.71055	-88.36311	1606	917	431	47
HSW2L2_FP1088_B0423_W_1589_50_P_V_809	28.72323	-88.36140	1589	885	392	44
HSW2L2_FP1090_B0423_W_1539_50_P_Y_827	28.73484	-88.37786	1539	24240	21720	90
HSW2L2_FP0092_B0423_W_1584_50_P_U_853	28.72634	-88.35132	1584	2332	854	37
HSW2L2_FP0093_B0423_W_1574_50_P_V_861	28.73225	-88.35915	1574	104490	83172	80
HSW2L2_FP0094_B0423_W_1543_50_P_W_870	28.73579	-88.36354	1543	266000	247238	93
HSW2L2_FP0095_B0424_W_1512_50_P_X_878	28.73942	-88.36812	1512	43710	35579	81
HSW2L2_FP1089_B0423_W_1580_50_P_W_818	28.72815	-88.36819	1580	1110	699	63